Coordination Chemistry Reviews 553 (2026) 217583

Contents lists available at ScienceDirect

Coordination Chemistry Reviews

journal homepage: www.elsevier.com/locate/ccr

Molecular devices based on the mechanical bond: recent advances☆,☆☆

Leonardo Andreoni [a,b], Chiara Taticchi [a,b], Brian Sachini [a,b], Alberto Credi [a,b,*]

[a] Dipartimento di Chimica Industriale "Toso Montanari", Alma Mater Studiorum – Università di Bologna, via Gobetti 85, 40129 Bologna, Italy
[b] Center for Light Activated Nanostructures, Institute for Organic Synthesis and Photoreactivity, National Research Council of Italy, via Gobetti 101, 40129 Bologna, Italy

ARTICLE INFO

Keywords:
Catenane
Chemical topology
Molecular knot
Molecular machine
Photochemistry
Rotaxane
Supramolecular chemistry

ABSTRACT

The bottom-up construction and operation of nanoscale devices – namely, multicomponent (supra)molecular architectures capable of performing functions beyond the reach of their individual components – constitute a central focus in nanoscience and a compelling challenge in nanotechnology. Over the past three decades, the development of artificial molecular devices, including molecular machines and motors, has continuously stimulated the creativity of chemists, and the field continues to evolve at a remarkable pace. Among the strategies employed, the mechanical bond has emerged as a particularly powerful means of connecting molecular components to build functional systems. Mechanically interlocked molecules uniquely combine the robustness of covalent frameworks with the dynamic properties of non-covalent assemblies. Moreover, the precise modulation of steric and electronic interactions between mechanically bonded components offers rich opportunities for the emergence of novel functions. Recent advances in the design and synthesis of rotaxanes, catenanes and related interlocked structures have enabled the construction and operation of increasingly complex molecular devices and materials, many of which are capable of executing well-defined tasks. In this review, we present selected examples – classified according to their functional outputs – that exemplify the progress and potential of this rapidly developing area over the past decade.

1. Molecular devices

In everyday life, we extensively use macroscopic devices, namely, objects or mechanisms specifically designed to serve a particular purpose or perform a defined function [1]. These devices typically consist of an assembly of components, each responsible for carrying out a simple task. Together, the components operate in a coordinated manner to produce a more complex and useful function characteristic of the device. For example, the operation of a hairdryer – producing a stream of hot air – results from the combined action of a switch, a heating element, and a fan, all connected via electrical wiring and housed within an appropriate framework.

This device paradigm can be extended to the molecular level [2,3]. A **molecular device** can be defined as an assembly of a discrete number of molecular components or subunits, each of which performs an individual function. The overall assembly thus executes a specific, more complex operation arising from the cooperative behavior of its parts. The actions of individual components may be quite elementary under a physico-chemical viewpoint, such as absorbing photons at specific wavelengths, transferring electrons, or forming hydrogen bonds. The growth of **supramolecular chemistry** [4,5], together with the progress of synthetic chemistry and the development of new methodologies for characterization of complex molecular species, have been instrumental for developing these concepts and transform them into real chemical systems. Coordination chemistry has also played a major role, not only because metal-ligand interactions underpin the synthesis and operation of numerous molecular devices reported to date [6–9], but also because modern coordination chemistry encompasses the binding of a wide variety of substrates – including cations, anions, neutral molecules, and nanomaterials – by diverse types of hosts [10–12], extending to heterogeneous systems such as surfaces, interfaces, and porous solids [13,14]. Therefore, as research has progressed, what initially represented a concept of primarily fundamental interest [15] has evolved into an approach with potential relevance to various technological and biomedical contexts, owing to development of innovative molecular-based systems and materials [16–20].

☆ This article is part of a Special issue entitled: 'Chemical Bonds' published in Coordination Chemistry Reviews.
☆☆ *Dedicated to Professor Giuseppe Resnati, celebrating a career in chemical bonds on the occasion of his 70th birthday.*

* Corresponding author at: Dipartimento di Chimica Industriale "Toso Montanari", Alma Mater Studiorum – Università di Bologna, via Gobetti 85, 40129 Bologna, Italy.
E-mail address: alberto.credi@unibo.it (A. Credi).

https://doi.org/10.1016/j.ccr.2026.217583
Received 31 October 2025; Received in revised form 19 December 2025; Accepted 5 January 2026
Available online 14 January 2026

Molecular devices are chemical systems and therefore operate through chemical reactions that typically involve both electronic and nuclear rearrangements. In some instances, the function relies primarily on electron or energy transfer, without significant changes in nuclear positions. In contrast, molecular machines and motors – a particular class of molecular devices – function through large-scale movements of molecular subunits or even entire components [2,21,22].

Molecular devices require energy to function, similarly to their macroscopic counterparts, as well as signals to interface with the operator [2,3,23]. The energy input can take the form of (*i*) a chemical reagent, (*ii*) absorbed photons, or (*iii*) addition/removal of electrons via electrochemical means [23,24]. Given the depletion of chemical fuels and growing environmental concerns, sunlight represents an ideal primary energy source [25], and processes that avoid the generation of waste products are especially desirable. Photoexcitation offers further advantages, including selectivity, reversibility, and precise spatiotemporal control [26].

To control and monitor the operation of a molecular device, an appropriate signal is necessary. Since at least one molecular component undergoes a state change during function, any observable signal associated with that change can be utilized. A variety of chemical and physical techniques are available for this purpose [2,21,22,27,28]. Typically, a device operates cyclically, making chemical stability and reset capability essential. This requirement implies that any chemical reaction involved in its function must be, at least to a reasonable extent, reversible. This condition is generally well satisfied by processes such as energy transfer, electron transfer (redox), proton transfer (acid–base), some photoreactions (e.g. photoisomerization), and certain metal–ligand coordination reactions.

The functions that molecular devices could perform are diverse. These include the transfer and processing of physical or chemical signals (e.g., switching, storing), energy conversion (e.g., converting light into chemical or electrical energy), catalysis, and a broad range of mechanical-like tasks – both at the molecular level (e.g., cargo transport across membranes) and in the micro- or macroscopic realm (e.g., development of materials for mechanical actuation).

2. The mechanical bond

In chemistry, a **mechanical bond** is defined [29,30] as a spatial entanglement in space between two or more molecular entities such that they cannot be separated without breaking or distorting chemical bonds between atoms. It is therefore a connection between molecular components: unlike conventional chemical bonds, it cannot occur between atoms. As such, the mechanical bond can be regarded as a specialized tool for the molecular bottom-up approach to constructing nanoscale structures, which is a primary chemical route toward nanotechnology [2–15,31]. Although mechanical bonds share certain features with chemical bonds – for instance, their formation may involve entropic changes – they are fundamentally different in nature. Rather than arising from patterns of electrostatic interactions involving electrons and nuclei, the mechanical bond is more akin to a physical link between material objects. Consequently, it lacks an intrinsic bond energy and is, in principle, roughly as strong as the weakest chemical bond that contributes to the constitution of the entangled molecular components.

Mechanical linkages are not only pervasive in natural and artificial macroscopic objects, where they enable unique properties and functions, but are also common in the biomolecular domain [32]. Despite this fact, a systematic understanding and control of mechanical bonding at the molecular level has only emerged in the past four decades [33]. This research field is closely related to **chemical topology** [34–36], which tackles the formidable challenge of making molecules with non-planar graphs – i.e., structures that cannot be represented on a sheet of paper without crossing points, even if bond lengths and angles are deformed at will. The difficulty in preparing such molecular architectures [37,38] lies in the need to generate, during the synthetic process, the specific entanglements and crossovers that ultimately result in the formation of mechanical bonds [39].

A detailed analysis of the methodologies developed to interlock molecular components via mechanical bonds is beyond the scope of this review [29]. However, it can be briefly recalled that current state-of-the-art approaches operate under either:

(a) thermodynamic control – using intermolecular binding strategies to arrange the component parts in stable structures that are prodromic to the formation of the entanglement (**template-directed synthesis**) [40–42]; or
(b) kinetic control, in which transition states are stabilized to render reactions that yield mechanically interlocked products faster than other competing pathways (**active template synthesis**) [43,44].

In thermodynamically controlled synthesis, the reactants are preorganized via noncovalent forces or coordination bonds which, in most instances, are retained in the final interlocked species. This can be an advantage because these interactions can be externally modulated post-synthetically to impart functionality. In some cases, the template agent – a molecule or ion – is not part of the interlocking components and may be removed at a later stage. Self-sorting strategies can also be exploited to obtain specific intertwined structures from a library of assembling subcomponents [45]. Conversely, kinetically controlled strategies do not require complementary binding motifs between components or their precursors, allowing access to interlocked structures where the components may not interact at all – such as in the so-called 'impossible' rotaxanes [46]. Chemical modification of the molecular components after they have been interlocked is also possible [47,48]; in such a case, the mechanical bond(s) needs to be preserved during the successive synthetic reactions. It has been shown very recently that the entanglement necessary to achieve mechanical bonding can be generated by a light-driven molecular rotary motor that winds molecular strands into discrete braided structures, without the need of templating or assembling processes [49].

The two main structural motifs arising from mechanical bonding in synthetic chemistry are catenanes and rotaxanes, both belonging to the broader family of **Mechanically Interlocked Molecules (MIMs)** [29,50]. A **catenane** (Fig. 1a) comprises at least two interlocked macrocyclic (ring-shaped) molecules. The simplest example is a [2]catenane (where the bracketed number denotes the number of interlocked components): a pair of interlocked molecular rings forming a chain, which epitomizes the mechanical bond. A **rotaxane** (Fig. 1b) – from latin *rota*, wheel, and *axis*, axle – consists of at least one macrocycle – the wheel – threaded by at least one thread-like molecule – the axle – whose extremities are capped with bulky substituents (stoppers) that prevent the macrocycle from slipping off. A [2]rotaxane – a molecular ring threaded by a dumbbell-shaped axle – is a particularly common type of MIM. Numerous other MIMs derived from catenanes and/or rotaxanes have been synthesized and investigated (Fig. 1c), and many more can be envisioned on geometrical grounds, presenting ongoing challenges for the ingenuity of synthetic chemists.

It should be noted, however, that MIMs are not always topologically complex, nor do they necessarily contain mechanical bonds. For example, [2]rotaxanes are topologically trivial, as the wheel and axle components could, in principle, be dissociated by stretching the bonds of the macrocycle until it passes over the stopper (this transformation is allowed in topology). Conversely, molecular knots – an intriguing subclass of MIMs – can exhibit entanglement without comprising distinguishable molecular components, and thus lack mechanical bonds [35]. A trefoil knot, for instance, is a single macrocyclic ring arranged into a knotted topology with three crossing points; such a configuration is topologically distinct from the same unknotted macrocycle (interconversion would require bond breaking or crossing, both unpermitted in topology), yet it does not involve mechanically bound molecular components. In this review, we will thus focus on MIMs that feature

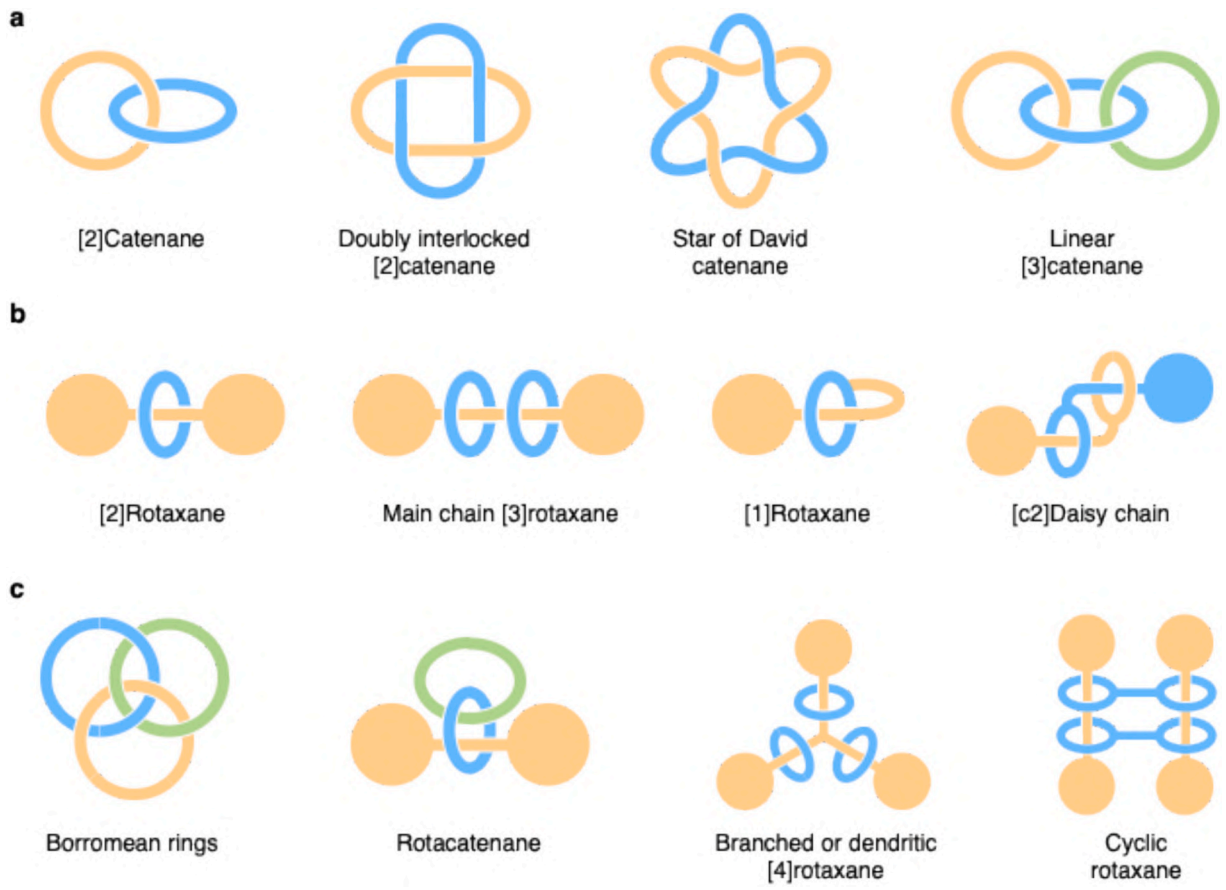

Fig. 1. Schematic drawing of molecular catenane (a) and rotaxane (b) architectures; more complex topologies and composite structures are shown in (c).

mechanical bonds, such as rotaxanes, catenanes and related species. For a discussion on molecular topology and knots, the interested reader can refer to exhaustive reviews on the subject [35,51].

3. Structural and dynamic consequences of mechanical bonding

As discussed above, mechanically bound molecular components may not engage in direct chemical interactions, yet they give rise to stable MIMs. This peculiar situation has several important implications for the structural properties and dynamic behavior of MIMs, distinguishing them from conventional molecules or supramolecular assemblies. Below is a (non-exhaustive) list of characteristics that are relevant for the present discussion. Molecular interlocking can:

- Enforce the proximity of molecular subunits that would not otherwise come into close spatial contact.
- Preserve the integrity of the assembly under a wide range of environmental conditions (e.g., solvent, temperature, pH, etc.).
- Enable the modulation (e.g. switching on/off) of intercomponent interactions without causing dissociation of the assembled parts.
- Affect the spatial arrangement of the component parts, giving rise to novel and unique stereochemical properties.
- Reduce the symmetry of the MIM relative to that of the individual molecular components; for example, MIMs that are chiral only by virtue of their topology can exist.
- Permit conformational, configurational or large-amplitude (co-conformational) movements of the interlocked parts while maintaining the integrity of the assembly.
- Restrict, or even completely suppress, certain degrees of freedom in the motion of the components.

These general features underscore how the mechanical bond introduces an entirely new dimension to molecular design and function and are particularly relevant for the realization of artificial **molecular devices and machines**.

In biological systems, **self-assembly** and **self-organization** are dominant processes for creating functional molecular-scale architectures; a paradigmatic example is provided by the light-harvesting antennas of bacterial photosynthesis, which form through the spontaneous assembly and spatial arrangement of numerous molecular units [52]. It is striking how Nature can harness weak intermolecular interactions to construct highly sophisticated supramolecular architectures. In an analogous way, creating artificial supramolecular systems through self-organization demands molecular components that are properly 'programmed' and a fine control over all weak interactions, including those with the solvent, so that the system is thermodynamically steered toward the intended structure. Achieving this goal is possible through the meticulous chemical design of the building blocks, as witnessed by the successful synthesis of complex multicomponent structures (e.g., molecular helicates [53], cages [54], knots [55], capsules [56], polyedra [57]) by self-organization of molecular components. Nevertheless, building artificial molecular devices via self-assembly and self-organization is far more challenging. The individual components must be designed not only to assemble spontaneously into a precise supramolecular architecture, but also to integrate their functions in a way consistent with the specific operation that the device or machine is meant to perform. In addition, supramolecular assemblies held together only by weak noncovalent interactions tend to be fragile and can readily fall apart when exposed to external perturbations such as change of solvent, pH or temperature. While this property can be exploited for obtaining specific functions [58], in most cases the device is not intended to disassemble in response to environmental changes.

For these reasons, the introduction of mechanical bonds between molecular components, enabled by the advanced techniques of modern synthetic chemistry, is an appealing and powerful strategy for constructing robust artificial molecular devices [59]. This approach may also serve as an alternative or complement to intercomponent connections based on classical bonds (e.g., covalent, coordination), which has traditionally been the primary method to obtain multicomponent species [2,60,61]. The following examples, organized according to the task performed rather than by MIM type, have been selected to illustrate the degree of structural and functional sophistication achieved by molecular devices constructed from interlocked component parts, and to showcase the opportunities offered by the mechanical bond in the bottom-up approach to molecular nanotechnology.

4. Light harvesting

The efficient absorption of light by molecular species is the first step of any process aimed at exploiting solar energy – including natural photosynthesis [62]. In artificial photosynthesis research, light-harvesting compounds are typically realized by gathering together (by self-assembly or covalent bonding) several chromophores and organizing them in such a way that the electronic excitation energy generated upon photon capture is transferred to a specific site where it could be utilized to drive a chemical reaction [63,64]. Dendrimers – three-dimensional macromolecular species characterized by a highly branched structure – represent appealing chemical scaffolds for this purpose [65,66], and coordination chemistry has been central for their development [67]. Making dendrimers with mechanically interlocked components – namely, rotaxane dendrimers, or dendritic rotaxanes – has been intriguing chemists for a long time [68,69,70]. However, it is only recently, owing to the progress in the controlled synthesis of both dendrimers and MIMs, that dendrimers of high generation and/or with a high density of mechanical bonds have become a reality [71,72]. Fig. 2 shows schematically different types of rotaxane dendrimers, depending on whether the mechanical bonds are located in the dendrimer core (type I), in the periphery (type II) or in the branches (type III).

A remarkable example of a light harvesting rotaxane dendrimer is shown in Fig. 3 [73]. This third-generation dendrimer possesses eight anthracene and twenty-four tetraphenylethene (TPE) energy donor units arranged around a central pyrene unit, which serves as the energy acceptor. The dynamic switching capability of the device is rooted in the pillar[5]arene macrocyclic components of the rotaxane moieties. These macrocycles are strategically positioned over urea groups that serve as stimuli-responsive binding stations. The mechanism involves the addition of water, that weakens the hydrogen bonding network. As a consequence, the macrocycle shifts its position toward the alkyl chain, resulting in the contraction of the overall dendrimer structure – a process confirmed through ^{1}H-NMR titration experiments. Water was also used as a 'bad' solvent to investigate aggregation-induced emission (AIE) phenomena. The formation of an aggregated state upon increasing

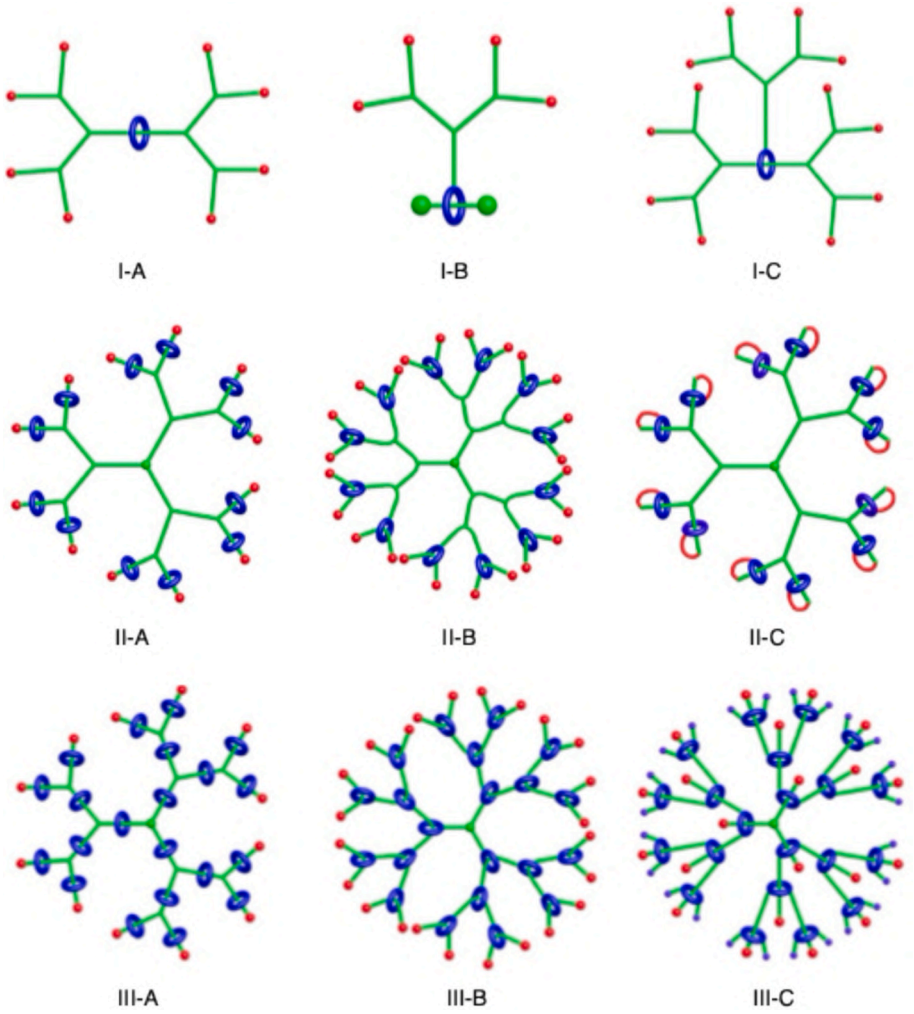

Fig. 2. Schematization of rotaxane dendrimers with mechanical bond(s) located in the core (I), in the periphery (II) or in the branches (III). The labels A, B and C mean respectively that the dendrons are covalently linked either to the axle(s), to the macrocycle(s) or to both. Reproduced with permission from Ref. [72] © 2021 American Chemical Society.

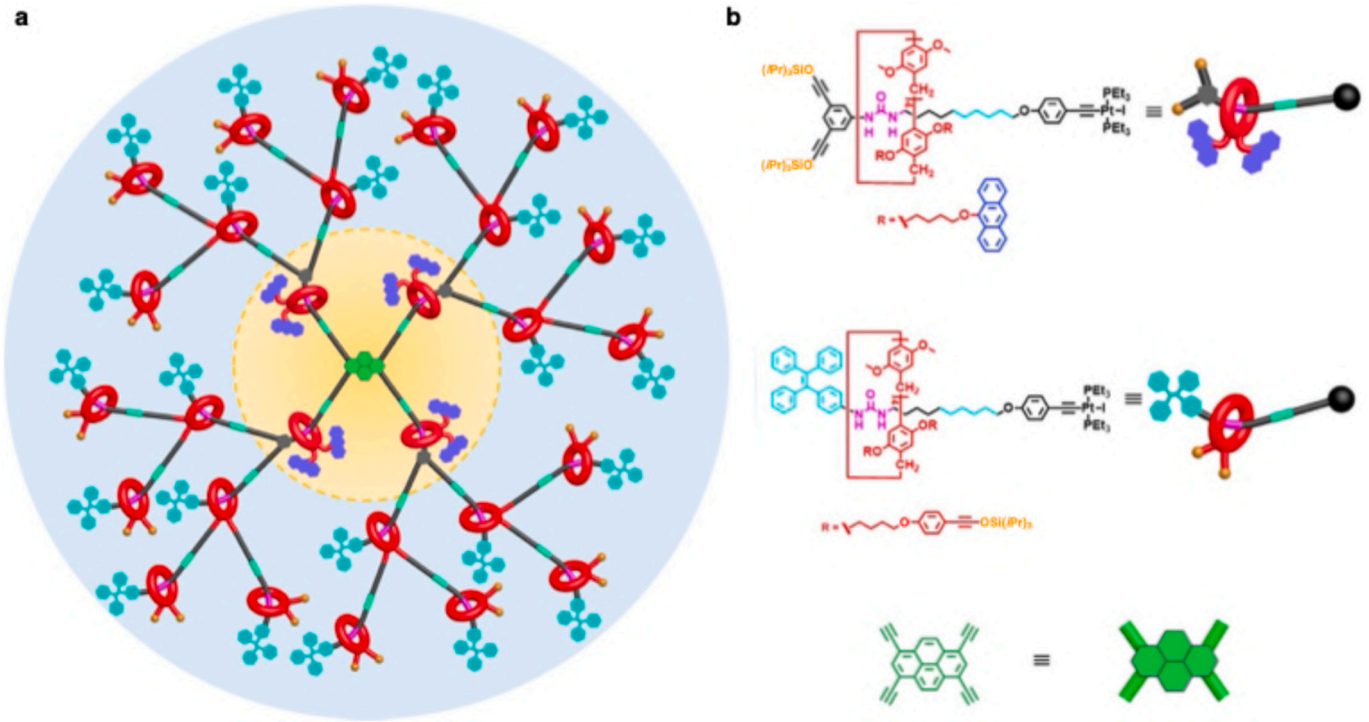

Fig. 3. (a) Schematic representation of a light-harvesting rotaxane dendrimer of third generation, containing tetraphenylethene and anthracene units as energy donors and a central pyrene moiety as the energy acceptor. (b) Structure formulas and cartoons of the building blocks, which are connected together by Cu-catalyzed alkyne coupling to yield the dendrimer by a divergent approach. Adapted with permission from Ref. [73] © 2022 Elsevier.

the water content of the solvent mixture was confirmed by dynamic light scattering and transmission electron microscopy experiments, setting the foundation for photophysical investigations.

A prerequisite for light harvesting is the overlap between the emission band of the donors and the absorption band of the pyrene acceptor. Fluorescence measurements in tetrahydrofuran revealed a high pyrene fluorescence and the absence of TPE and anthracene peaks. Sequential addition of water led to a notable increase in emission, with a maximum for 80% water content. In mixtures exceeding 80% water, the fluorescence was gradually quenched. This behavior highlights a competition between AIE and aggregation-caused quenching (ACQ) effects. The energy transfer pathway and dynamics were further investigated by means of fluorescence decay analysis.

Overall, this compound exhibits a strong light-harvesting ability and an enhanced antenna effect. A comparison with analogous first- and second-generation dendrimers shows that both behaviors improve upon increasing the generation, rendering them promising blueprints for real-world applications.

MIMs can be exploited to suppress unwanted photophysical decay pathways, guiding the evolution of the excited state towards the desired mechanism. For instance, two rotaxanes exhibiting light-induced energy transfer were recently reported [74]. They consist of a linear axle with two bulky porphyrin donors positioned on either side of a central fullerene acceptor, which in turn is surrounded by either a [10]cycloparaphenylene (CPP) nanohoop or an aza-[10]CPP analogue. Transient absorption spectroscopy experiments performed on the rotaxanes in the femto- and nanosecond time scales provided evidence for the formation of the lowest triplet excited state of the fullerene moiety. Control experiments performed on the non-interlocked axle exhibited a markedly different outcome: in this compound photoexcitation resulted in charge separation, as confirmed by the detection of the fullerene radical anion. These results clearly demonstrate the ability of the CPP nanohoops to suppress the charge transfer pathway in favor of efficient triplet-triplet energy transfer from the porphyrin chromophores to the fullerene unit. Interestingly, both the photoreaction mechanism and light harvesting efficiency seem to be unaffected by the different constitution of the nanohoops [74].

The mechanical bond can also provide the precise spatial proximity necessary to maximize efficiency in charge separation, as illustrated by a recently described [2]catenane [75]. The MIM is assembled from two strongly electron-poor chromophores: a perylene diimide derivative that acts as the light-absorbing donor component, and a pyridinium-based cyclophane that acts as the acceptor macrocycle. The mechanical bond forces the two rings to assume a tight arrangement that promotes a strong π-electronic coupling, as confirmed by bathochromic shifts in the UV-visible spectra. Owing to this unique topology, the system can achieve ultrafast charge separation despite a relatively low thermodynamic driving force [75]. At the same time, the (co-)conformational properties of the catenane allowed a significant prolongation of the lifetime of the charge-separated state. This dual kinetic and thermodynamic control was translated into a functional application: the catenane displayed more than a two-fold enhancement in efficiency for the photocatalytic selective oxidation of aryl sulfides compared with systems lacking a mechanical bond. This improvement arises from utilization of the high-energy charge-separated state, underscoring the potential of the catenane as a low-energy-loss blueprint for energy conversion.

In summary, the evolution of mechanically interlocked light-harvesting systems – from early rotaxane dendrimers to more recent examples such as those discussed above – highlights the maturation of MIMs as advanced molecular scaffolds. Collectively, these studies demonstrate that mechanical bonds can enable, suppress, or finely tune the key steps of solar energy conversion, offering a versatile framework for the design of future photocatalytic and solar fuel systems.

5. Molecular recognition

The design of host architectures that can strongly and selectively recognize a wide range of molecular or ionic species relevant to biology, medicine, and the environment has been attracting much attention [5] and remains a hot topic of contemporary chemical research [76]. MIMs

such as rotaxanes and catenanes have been shown to provide highly effective recognition environments, owing to their unique three-dimensional, topologically preorganized cavities [77]. Numerous examples of MIMs with cation [78] and anion [79] binding properties have been reported in the literature. The advantages offered by mechanically bound molecular components as receptors, in comparison with conventional acyclic or macrocyclic hosts, are particularly evident in the recognition of ion pairs (Fig. 4).

Heteroditopic homo[2]catenanes incorporating oligo(ethylene glycol) units for alkali metal cation binding and halogen-bond donor groups for anion recognition (Fig. 5a) were synthesized using a metal-template approach. NMR binding experiments revealed that the interlocked hosts display a substantially higher affinity for cations than the corresponding parent macrocycles. Solid-state data further showed that cation binding induces notable conformational flexibility within the structures. Moreover, the inherently weak halide affinities of the neutral [2]catenanes increased markedly upon pre-complexation with alkali metal cations, reflecting cooperative electrostatic effects relevant to ion-pair recognition. The ability of these compounds to act as extractants of alkali halide salts was further illustrated through solid-liquid extraction studies, underscoring the potential of mechanical bonds in designing new receptors for ion-pair recognition and extraction [80].

Very recently, a new class of rotaxanes capable of recognizing both anions and cations using the same donor atoms through chalcogen and halogen bonding was reported [81]. These amphoteric hosts (Fig. 5b) possess anisotropically polarized tellurium and/or iodine atoms, which can act as Lewis acids to bind anions or as Lewis bases to coordinate metal cations. This work is important because, by exploiting and extending key concepts of coordination compounds [10–12,82,83], it introduces a single-platform strategy for ion sensing, thus representing a major advance in supramolecular host-guest chemistry and the design of multifunctional recognition systems.

The introduction of molecular photoswitches in the components of rotaxane and catenane hosts can enable light control of ion complexation. For example, photoswitchable chloride receptors based on a rotaxane (Fig. 5c) [84] or a catenane [85] were constructed by incorporating a stiff stilbene photoswitch in one macrocyclic component. In these systems, the *Z*-*E* photoisomerization of the stiff stilbene units alters the geometry of the macrocycle, modulating the affinity for chloride of the whole MIM. The *E* isomer displays a lower binding constant compared to the *Z* isomer (up to 12 times); as the irradiation at different wavelengths allows to control the ratio between the *E* and *Z* isomer, the uptake and release of chloride can be controlled with a light stimulus.

6. Mechanical switching of chirality and chiroptical properties

As pointed out in the introduction, the mechanical bond in rotaxanes and catenanes allows extensive rearrangements of the molecular components, which can be induced and controlled by modulating the interactions between them. This is usually achieved by chemical, electrochemical or photochemical switching of specific subunits in the components. Therefore, such transformations cause large amplitude (on the molecular scale) movements which are at the basis of mechanical switching processes. The most common realizations of this idea with rotaxanes and catenanes are the bistable mechanical switches schematically illustrated in Fig. 6. In a [2]rotaxane such as that shown in Fig. 6a, the ring is displaced reversibly between two non-equivalent recognition sites (the 'stations') located along the dumbbell-shaped component by external stimuli, yielding a controllable molecular shuttle [86–91]. Fig. 6b depicts a similar design based on a [2]catenane [92,93]. Many examples of systems of this kind have been reported in the past three decades [2,21,22,29,86–93], including their evolution into MIMs more sophisticated than [2]rotaxanes and [2]catenanes [94,95].

In recent years the focus of research on MIM-based switches has gradually shifted from the fundamental understanding of mechanical switching in different environments to new properties and applications resulting from its exploitation [96]. For example, the rotaxane shown in Fig. 7a can be reversibly switched between prochiral and mechanically planar chiral forms by acid-base reactions [97]. As mentioned in the introduction, a MIM can exhibit chirality even though its individual components are not chiral; this happens when the improper symmetry operations of the separated components are not symmetry operations of the whole [98]. Compounds of this kind are referred to as 'mechanically chiral' because the stereogenic element is the mechanical bond itself, together with the underlying symmetry properties of the covalent components. The rotaxane in Fig. 7a consists of a ring with C_{1h} symmetry – i.e., with only a mirror plane parallel to the macrocycle plane – and a highly symmetric (D_{2h}) axle with two identical extremities. In the starting (acidic) state the ring is positioned in the center of the axle, because of its strong preference for the dibenzylammonium station with respect to the much weaker triazolium binding sites. The rotaxane is thus achiral because it still possesses a mirror plane parallel to the macrocycle. However, deactivation of the ammonium station by deprotonation leads to the displacement of the macrocycle on one of the two equivalent triazolium sites, causing a reduction of symmetry and the appearance of mechanical chirality. The existence of two enantiomeric forms in the chiral state was confirmed experimentally by the observation of single sets of resonances in the ^{1}H-NMR spectrum, and the thermally driven ring shuttling between the two equivalent triazolium stations – responsible for inversion of the stereogenic element – was quantitatively examined through variable temperature ^{1}H-NMR experiments. The rotaxane can be brought back to the achiral form by regeneration of the ammonium station upon addition of an acid

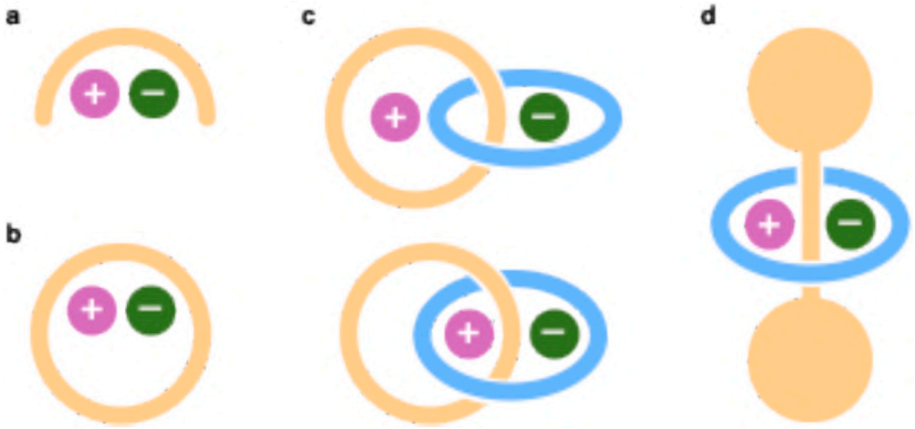

Fig. 4. Schematic comparison of ion-pair recognition by heteroditopic receptors: acyclic species (a), macrocycle (b), catenane (c) and rotaxane (d).

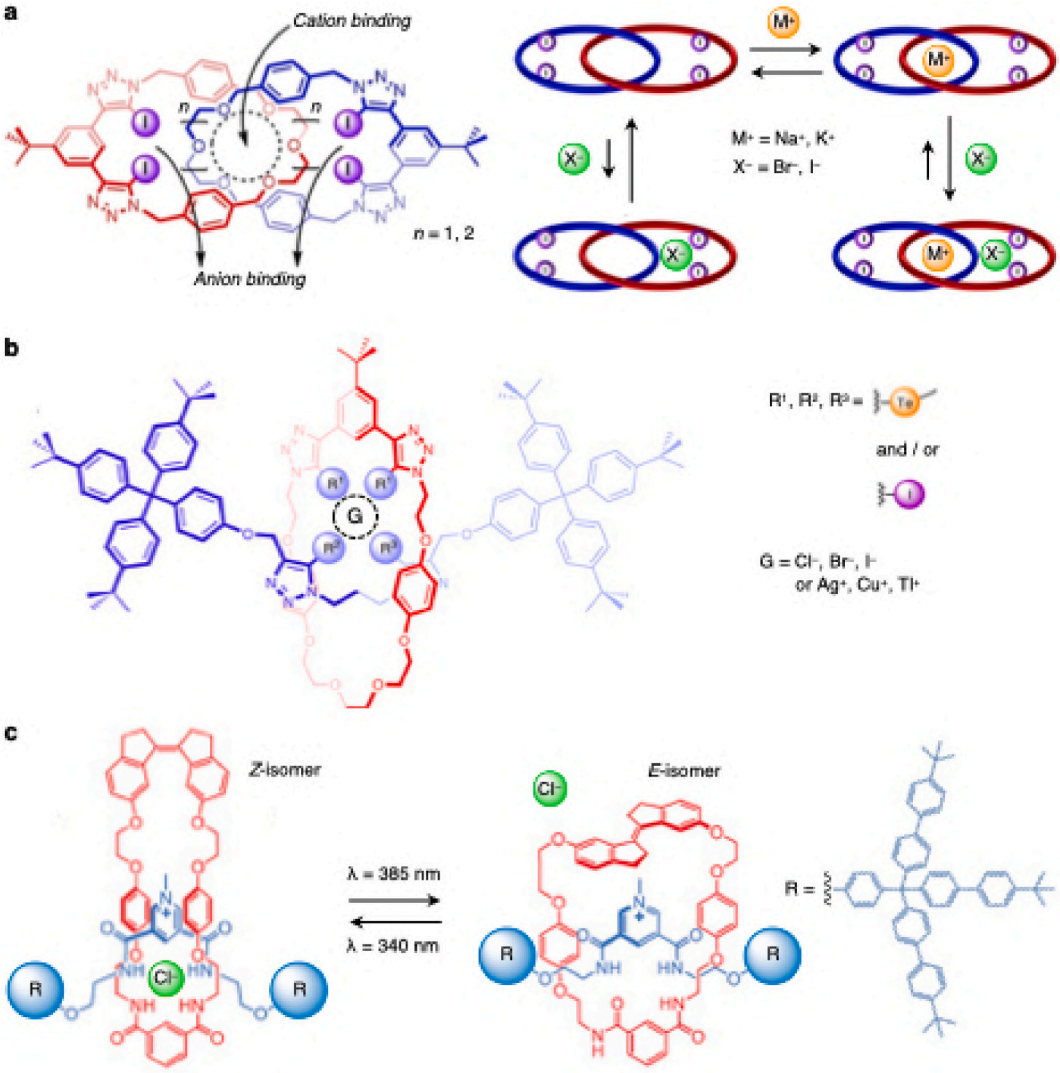

Fig. 5. Examples of MIM-based hosts for ionic species. (a) Structure formula (left) and schematic operation (right) of heteroditopic [2]catenanes ion pair receptors. Adapted from Ref. [80] © 2023 The Authors. (b) Structure formula of amphoteric rotaxanes capable of recognizing both anions and cations by chalcogen and halogen bonding. Adapted from Ref. [81] © 2025 The Authors. (c) Light-induced switching of chloride recognition by a [2]rotaxane bearing a photoactive macrocyclic component [84].

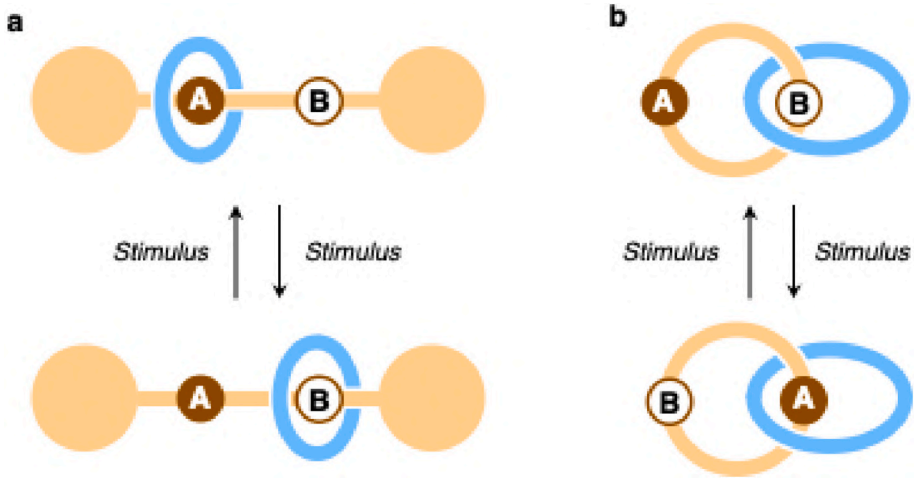

Fig. 6. Schematization of bistable mechanical switches based on stimuli-responsive (a) [2]rotaxane (molecular shuttle) and (b) [2]catenane structures.

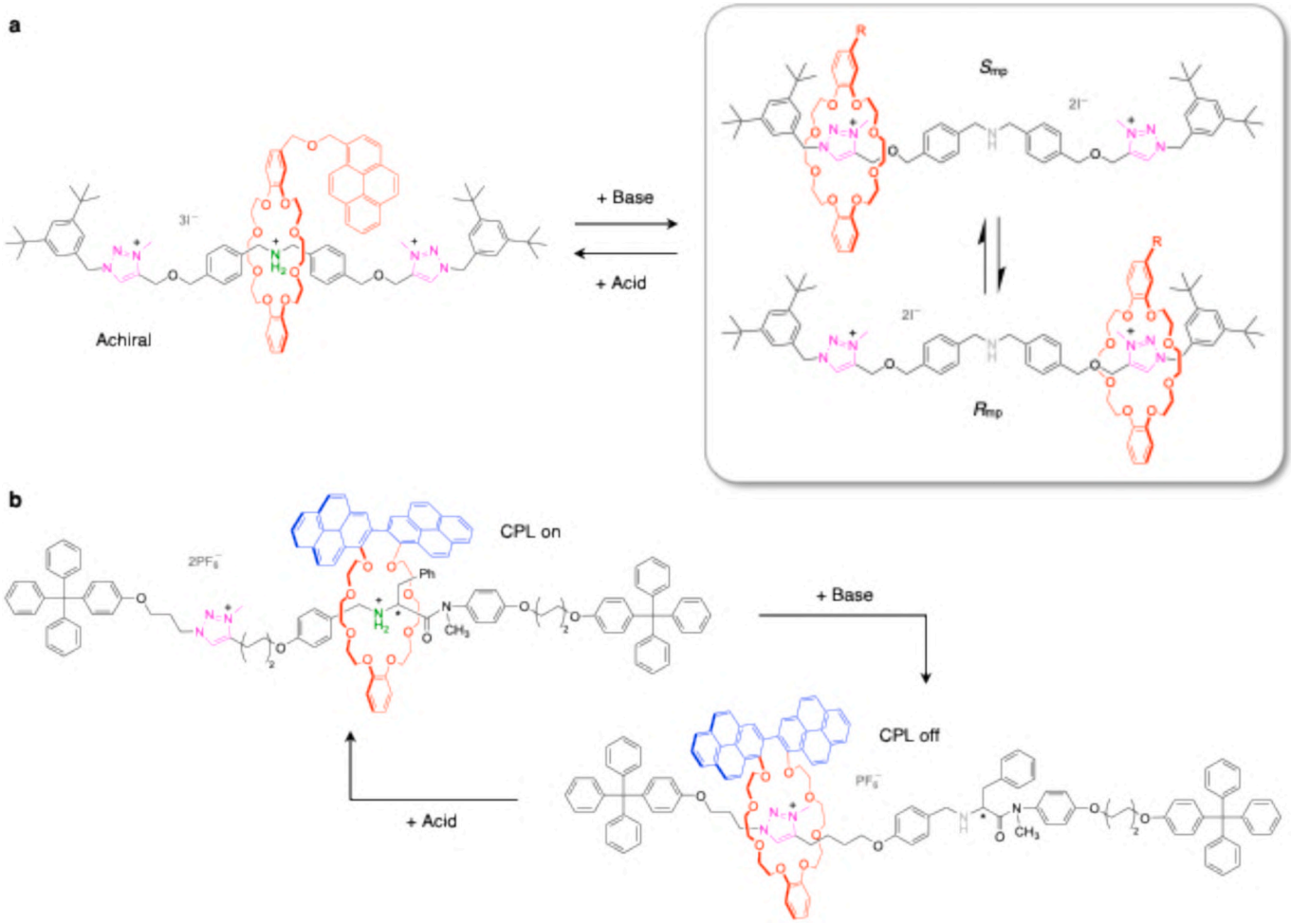

Fig. 7. (a) A [2]rotaxane in which mechanically planar chirality can be switched on and off by the acid-base-induced displacement of the macrocycle along the axle [97]. The thermally driven shuttling of the ring between the two equivalent triazolium stations causes the interconversion of the two mechanically planar enantiomers R_{mp} and S_{mp}. (b) Schematization of the on-off switching of the CPL emission in a [2]rotaxane, resulting from the modulation of chiral information transfer from the axle to the luminescent macrocycle, which in turn is controlled by the acid-base-induced motion of the latter along the former [100].

(Fig. 7a). The population of the two enantiomeric co-conformations in the chiral state can be unbalanced by the interaction of the positively charged rotaxane with optically active anions, potentially disclosing new strategies for enantioselective sensing and catalysis [97].

Mechanical chirality in MIMs can provide novel directions to investigate chiroptical properties, namely, optical properties arising from the interaction between chiral structures and circularly polarized light [99]. Chiroptical phenomena are of interest for the development of advanced photonic materials, sensing technologies and drug discovery. Fig. 7b illustrates the first example of on-off switching of circularly polarized luminescence (CPL) in an acid-base controllable molecular shuttle [100]. The origin of the chiroptical behavior lies in the transfer of chirality from a secondary ammonium station that incorporates either D- or L-phenylalanine residues functioning as covalent stereogenic elements to an achiral crown ether macrocycle that carries a luminescent 2,2'-bipyrene unit. In the protonated state the macrocycle encircles the ammonium site, where it experiences the chiral environment created by the phenylalanine residue which, in turn, induces a preferential spatial arrangement of the two pyrene moieties of the 2,2'-bipyrene unit, leading to CPL emission. Depending on the enantiomeric form of the axle, the macrocycle exhibits CPL signals of opposite handedness. Upon treatment with base, the macrocycle is displaced to the triazolium binding site, thereby disrupting the transfer of chiral information and suppressing the CPL response. The latter can be restored by acidification; remarkably, the total luminescence intensity and spectral profile are essentially preserved in both states.

In a related work, a topologically chiral [2]catenane endowed with two pyrenyl substituents – one for each molecular ring – was employed to obtain a three-state CPL switch (Fig. 8) [101]. The interaction between the two pyrenyl moieties, which is well known to give rise to excimer emission, was modulated by exploiting the ring rearrangements induced by chemical inputs such as Na^+ or H^+. As a consequence, the system could be reversibly switched between three states with different chiroptical properties: an initial 'closed' form with a low CPL emission, an 'open' form (in the presence of Na^+ cations) in which the CPL emission is essentially turned off, and a protonated form characterized with a high CPL signal. This conceptual approach to multistate CPL switches could provide a platform for the development of novel chiroptical materials.

7. Progressive ring shuttling

Progressive and directional linear motion over long distances is a characteristic feature of motor proteins like kinesin and myosin, that are capable of 'walking' along a track. In principle, this goal could be realized with rotaxane-based molecular shuttles by increasing the number of stations on the axle and precisely controlling their interaction with the macrocycle. However, although two-station rotaxanes are very well established, introducing additional, distinct interaction sites on the axle remains challenging. Full control of the ring movement requires: (a)

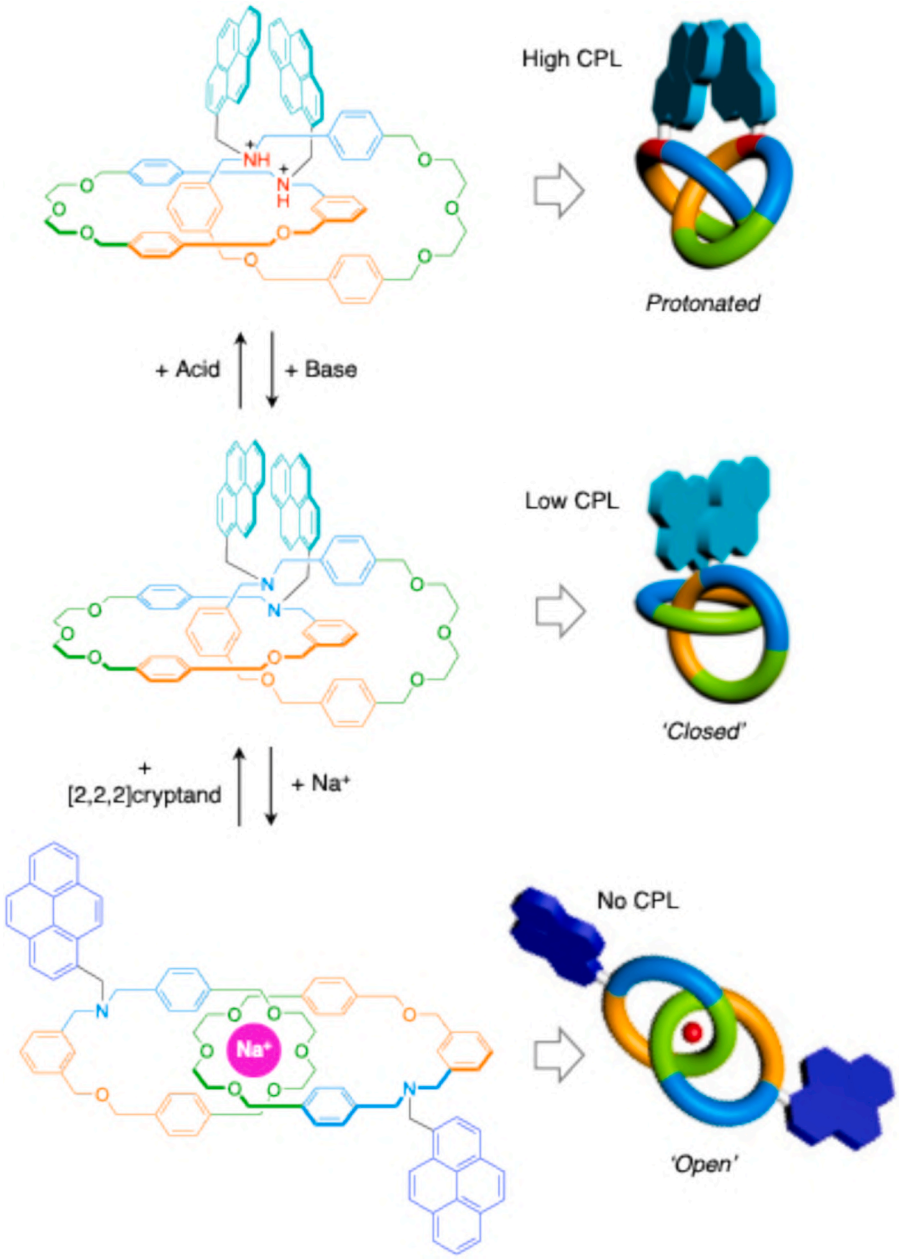

Fig. 8. Stimuli-induced three-state modulation of CPL in a topologically chiral [2]catenane. Adapted with permission from Ref. [101] © 2023 Wiley-VCH.

selective and mutually exclusive binding of the ring to each station, ensuring only one co-conformational isomer under given conditions; (b) independent, orthogonal stimuli to switch each station on or off; and (c) reversible switching reactions to permit cycling. Directional motion further demands a carefully designed sequence of stations along the axle. Three-station [2]rotaxanes are the logical next step toward progressive linear shuttles; yet, they remain rare, and only a few reported systems satisfy these stringent requirements [102,103].

A tristable mechanical switch based on a [2]rotaxane, in which the position of the macrocyclic ring with respect to three nonequivalent stations can be precisely controlled by external inputs, was recently described [104]. As shown in Fig. 9a, the molecular shuttle consists of a crown ether threaded by an axle comprising a secondary ammonium, a bipyridinium and a triazolium recognition site. Owing to the possibility to switch off-on (*i*) the ammonium station by chemical (base-acid) stimuli, and (*ii*) the bipyridinium station by electrochemical (red-ox) stimuli, the system can perform two sequential ring translation steps along the same direction upon application of two independent inputs (Fig. 9a). The position of the ring with respect to the stations on the axle can be determined, among other methods, by comparing the redox potential values corresponding to the reduction of the bipyridinium and triazolium units in various compounds (Fig. 9b). Specifically, the reduction potentials of both the bipyridinium and the triazolium stations are shifted to more negative values when they are encircled by the macrocycle. Thus, the data in the top two boxes of Fig. 9b indicate that at the beginning of the switching cycle the ring is located on the ammonium station. When the latter is switched off (either temporarily by addition of a base, or permanently by acylation), the macrocycle moves onto the bipyridinium station, whose reduction happens at more negative potential values (bottom two boxes in Fig. 9b, blue circles). In the deprotonated or acylated rotaxane the triazolium reduction is also negatively shifted (bottom two boxes in Fig. 9b, magenta circles): this observation suggests that, after the bipyridinium unit has been fully reduced, the triazolium station becomes encircled by the ring.

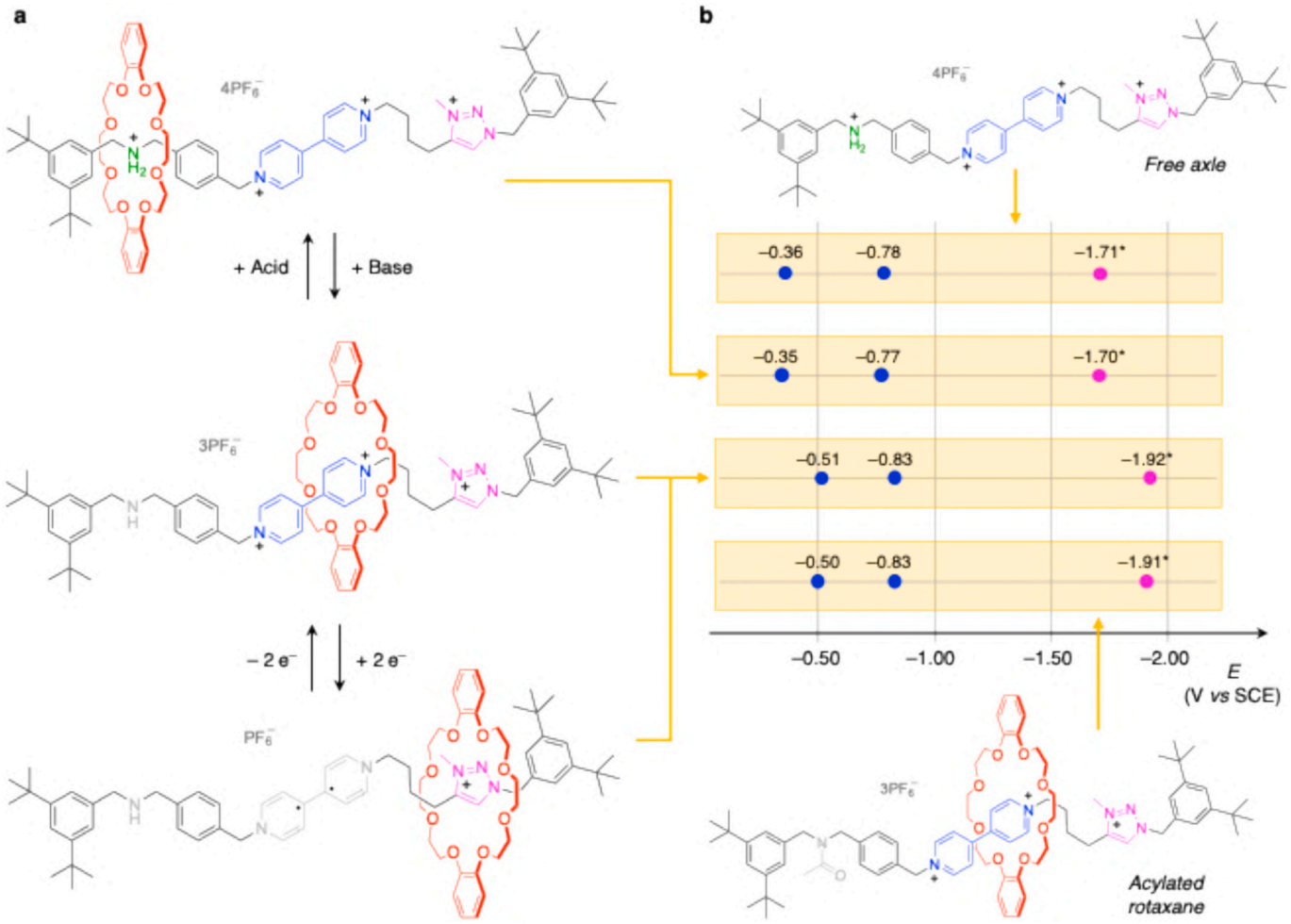

Fig. 9. (a) Structure formula and operation scheme of a [2]rotaxane in which the macrocyclic component can be precisely positioned around each of three nonequivalent stations by acid-base and redox stimuli [104]. (b) Comparison of the redox potential values of the rotaxane in its protonated and deprotonated states, together with those of the free axle and of a parent rotaxane in which the primary station is permanently switched off by acylation (CH_3CN, room temperature). Values marked with an asterisk correspond to peak potentials of poorly reversible processes; all other values are half-wave potentials of reversible processes. The colors of the points correspond to that of the electroactive units.

The excellent co-conformational selectivity in each state, combined with the clean, reversible and orthogonal nature of the two switching processes, make this design appealing for the construction of multistate devices that can respond to an array of inputs, such as molecular logic gates, and of linear molecular motors.

8. Gears

The synthesis and study of artificial structures in which different and distinct molecular movements can take place is a crucial step towards the development of nanoscale mechanical devices capable of transforming or transmitting motion [2,105]. If these movements are concerted – that is, synchronized – molecular gears could, in principle, be obtained [106,107]. To achieve this goal, two fundamental design principles, first investigated in early covalent systems, must be satisfied: mechanical coupling and kinetic fidelity [106]. For movement to be truly geared, the rotation of one component must be sterically or topologically constrained to induce a precise, corresponding motion in a second component, thereby enforcing a correlated motion between them. Crucially, the system must also exhibit kinetic fidelity: the correlated motion (gearing) has to be a low-energy pathway, while the competing, uncoupled motion (gear slippage) should require a high activation energy. This high barrier to slippage ensures the long-term conservation of the 'phase relationship' between the components, which is necessary for a stable, functional system.

Because of these requirements, the design of molecular gears is highly challenging, and examples of MIM-based molecular gears in which the mechanical bond is leveraged to couple the components motion are very rare. For instance, a recent investigation along this line involved the [2]rotaxane shown in Fig. 10a, consisting of a crown ether macrocycle surrounding an axle that contains two identical triazolium stations connected by a dibenzylamide moiety [108]. Because of the restricted rotation about the CN–CO bond of the amide, the rotaxane exists as a pair of *E/Z* diastereoisomers, which differ for the relative position of the macrocycle and the formyl moiety of the amide. A species of this kind can undergo *E-Z* isomerization according to three distinct mechanisms (Fig. 10b): (*i*) conformational isomerization through rotation about the CN–CO covalent bond of the amide 'rotor', (*ii*) co-conformational isomerization via translation of the macrocycle between the triazolium stations (provided that the central amide is not too bulky to prevent shuttling), and (*iii*) degenerate isomerization – that is, automerization – via concerted bond rotation and ring shuttling. The latter circumstance would correspond to geared rotary and translational movements. The rotaxane was thoroughly characterized by variable temperature and bidimensional NMR spectroscopies in different solvents, and the results showed that *E-Z* isomerization can occur by both covalent bond rotation (mechanism *i*) and ring shuttling (mechanism *ii*). Although the two motions are not concerted (i.e., mechanism *iii* was not

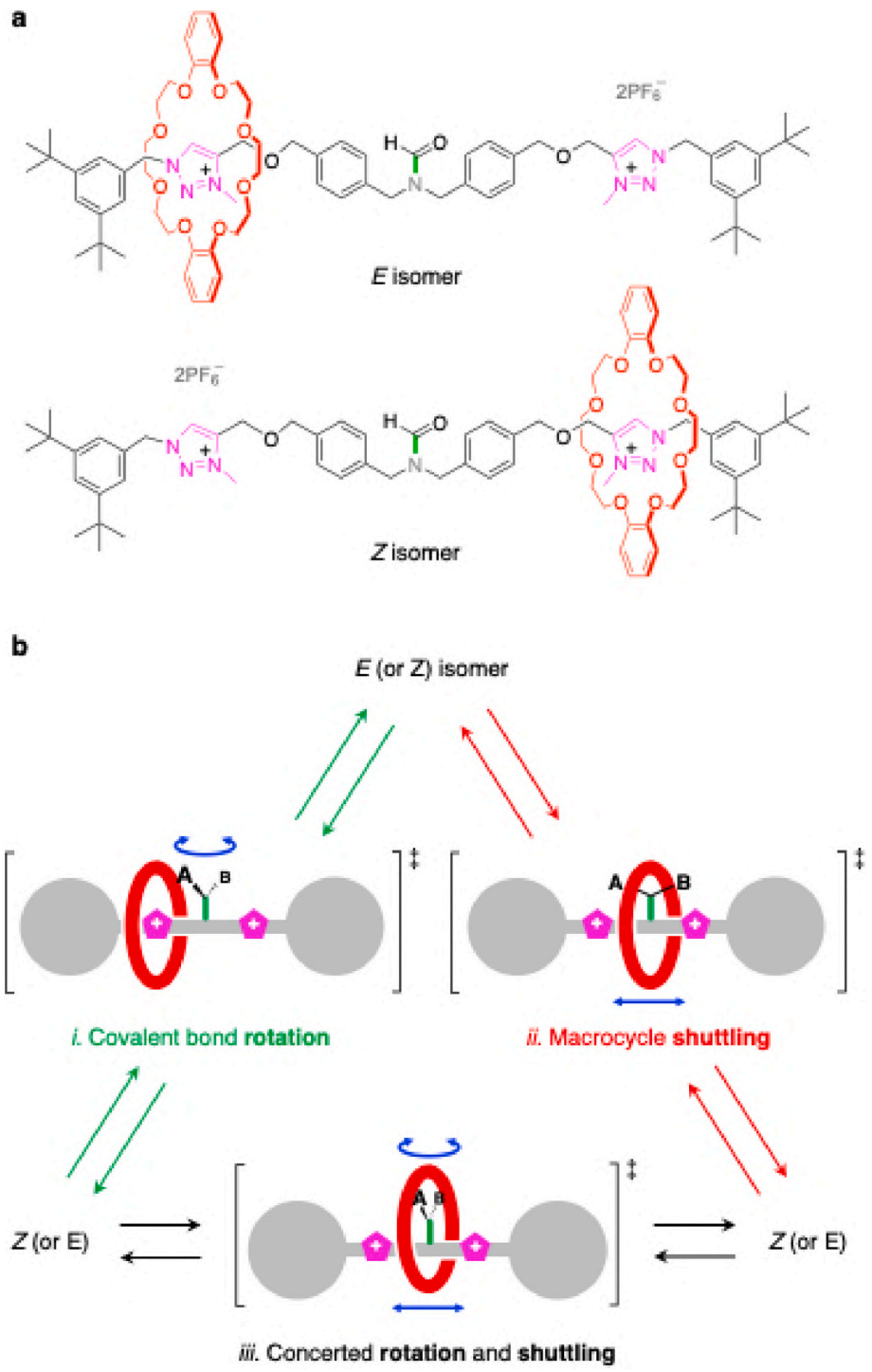

Fig. 10. (a) Structure formula of the *E* and *Z* isomers of a [2]rotaxane whose axle contains two identical macrocycle recognition sites bridged by an amide moiety [108]. (b) Schematics illustrating the possible *E-Z* isomerization pathways and simplified depictions of the corresponding transition states. The blue arrows indicate the associated molecular movements. While individual bond rotation or macrocycle shuttling result in a distinct stereoisomer, the concerted rotation-shuttling mechanism regenerates the original isomeric form.

observed), the concomitant occurrence of mechanically distinct and entirely different isomerization paths in the same molecule is an extremely rare event in chemistry and was never observed before in MIMs. Furthermore, the rates of the two movements are influenced oppositely by changes in solvent polarity: this behavior can be exploited to selectively control each process and regulate the relative contributions of the two mechanisms to the isomerization.

An outstanding example of correlated translational movements was reported for a [3]rotaxane consisting of two macrocyclic rings of different size that encircle a rigid axle with two identical stations (Fig. 11) [109]. Such a rotaxane is saturated, that is, all the recognition sites are complexed by a macrocycle; therefore, ring shuttling as depicted in Fig. 6a cannot occur. Variable temperature NMR experiments, however, demonstrated that in this compound the two macrocycles switch place simultaneously by passing the smaller ring through the larger one, thereby achieving ring-through-ring molecular shuttling.

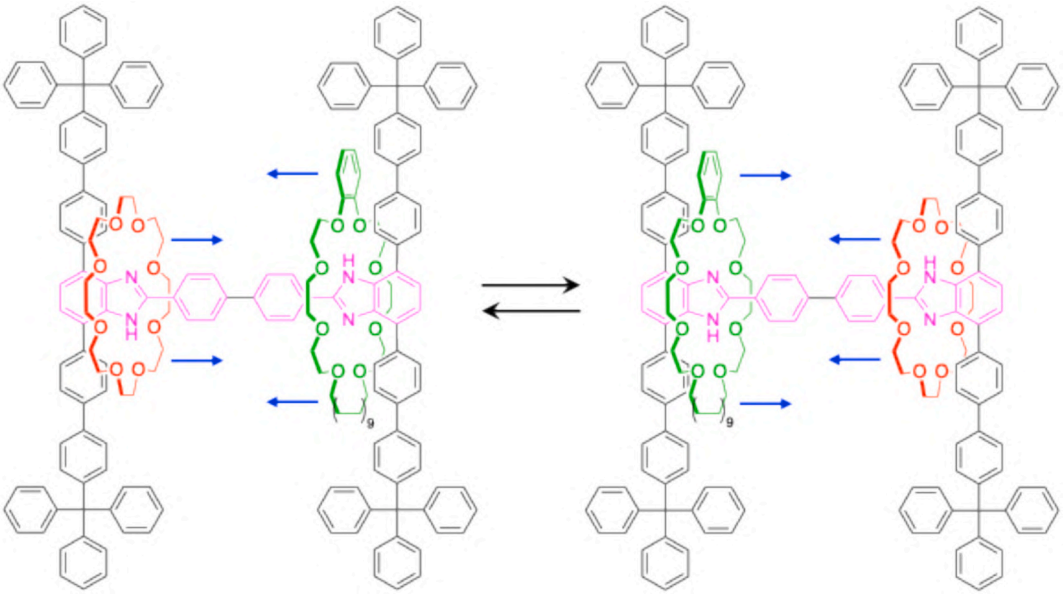

Fig. 11. Structure formula of a [3]rotaxane in which two interlocked macrocycles of different size switch place simultaneously according to a thermally activated ring-through-ring shuttling mechanism [109].

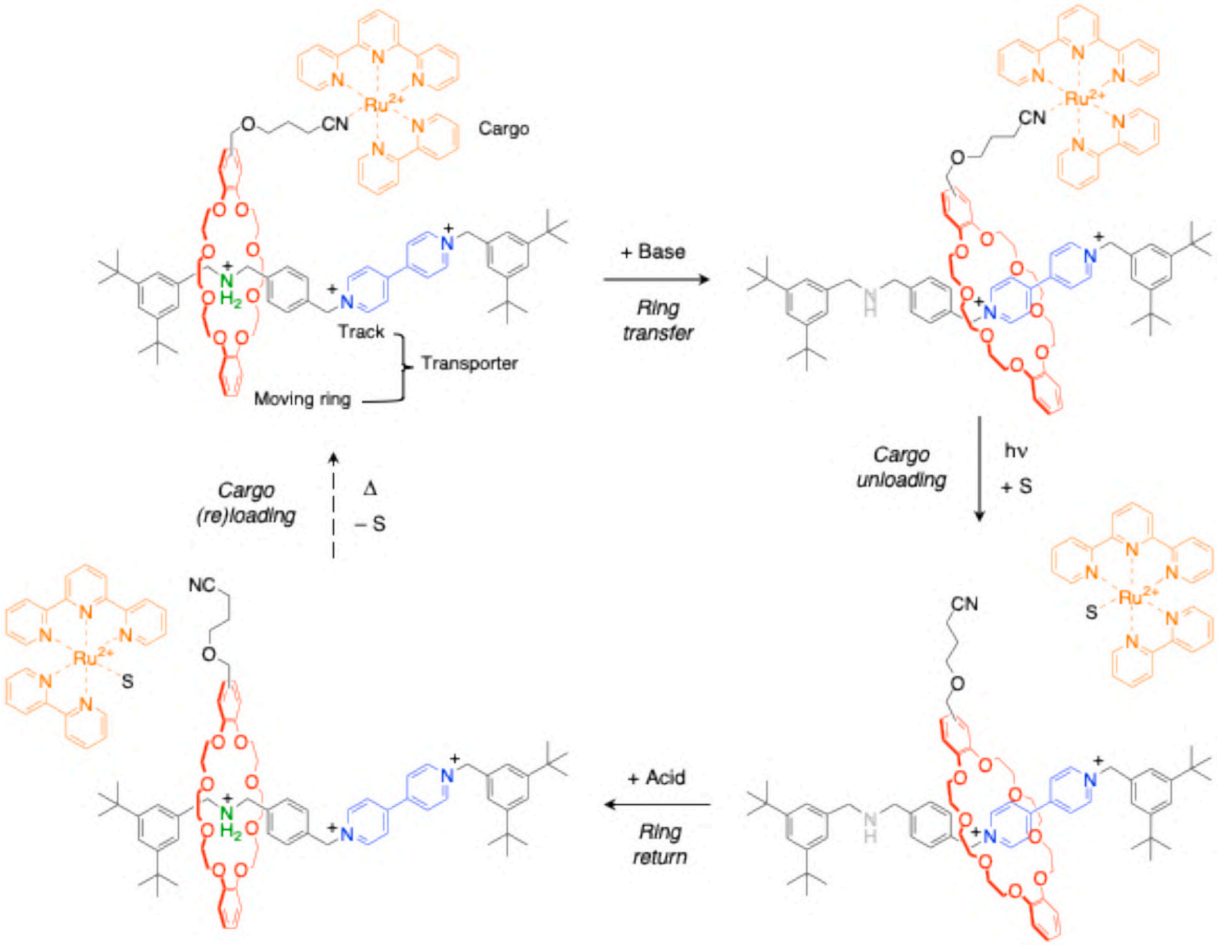

Fig. 12. Structure formula and operation of an artificial molecular transporter [114]. In this bistable [2]rotaxane, the macrocyclic component can be displaced between two stations on the axle by chemical inputs and is designed to release (photochemically) and collect (thermally) a Ruthenium complex as a molecular cargo; S is a solvent molecule.

A comparison with model [2]rotaxanes showed that this rearrangement is slower than shuttling of a single ring between the same two stations, because of additional enthalpic (steric) and entropic (organizational) costs associated with passing one ring through another. This study expands the range of dynamic phenomena that can occur at the molecular scale and highlights the level of sophistication of MIM-based mechanical devices.

The examples just discussed illustrate spontaneous (random) movements powered by thermal energy. It was shown that light-fueled molecular rotary motors can transmit their movement to connected 'passive' components, such as rotors [110] and shuttles [111]. The latter study concerns a rotary motor integrated with a [1]rotaxane architecture and shows that the photochemically induced unidirectional rotation of the motor drives the back-and-forth relative translation of the macrocycle and the axle, thus reminding a crank-slider mechanism.

9. Transporters

One of the key functions of biomolecular machinery is the directed transport of molecular or ionic species within cells and across membranes [52]. Therefore, the synthesis and operation of artificial (supra) molecular species that can transport substrates in a controlled manner is not only a challenging task in nanoscience but also a potential avenue towards new biomedical solutions and applications in catalysis, materials science and energy conversion [112,113].

Controllable molecular shuttles are appealing platforms to develop transporters because the translation of the macrocyclic component along the axle could be exploited to move a substrate; to this aim, the macrocycle should be equipped with a docking site capable of loading and unloading a molecular cargo. The operation of such a device must fulfil three requisites: (a) independent and orthogonal stimuli should be used respectively to move the macrocycle and to connect/disconnect the cargo; (b) the latter should remain bound to the transporter during the shuttling, and; (c) reversible switching processes should be employed. A [2]rotaxane designed to realize this idea is shown in Fig. 12 [114]. The axle component, which plays the role of a track, consists of an ammonium and a bipyridinium station for a crown ether, which in its turn is functionalized with a nitrile moiety coordinated to a $[Ru(tpy)(bpy)]^{2+}$ complex (tpy = 2,2':6',2"-terpyridine, bpy=2,2'-bipyridine). As illustrated schematically in Fig. 12, in the initial state the transporter has the metal complex attached to the macrocycle, which encircles the ammonium station. In acetonitrile, switching off the latter by deprotonation with a base triggers the movement of the (loaded) macrocycle towards the bipyridinium station. Successive irradiation with visible light induces the release of the cargo by photochemical de-coordination [115]. The addition of the acid restores the ammonium station and causes the return on the (unloaded) macrocycle at the starting position. Thermal re-coordination of the cargo on the macrocycle is expected to close the cycle; however, this process has not been observed in experiments, probably because the cyanide moiety on the rotaxane is unable to displace the ancillary ligand – most likely a solvent molecule – which in the meantime has taken the place in the Ru complex.

The system shown in Fig. 12 was investigated in homogeneous solution and is therefore a proof-of-concept study. To appreciate the effect of directed transport, the molecular device should be immobilized in some way – for example, deposited on a surface [116,117] – or inserted in a membrane [118]. An artificial molecular shuttle that can operate in a bilayer membrane and passively transport K^+ ions across it is shown in Fig. 13a [119]. It is a rotaxane designed to be incorporated into a bilayer in a membrane-spanning arrangement, owing to its amphiphilic nature and a length (about 3.2 nm) comparable to the thickness of a typical phospholipid bilayer. The axle component is symmetric and comprises two secondary ammonium units as the terminal stations for the shuttle, a central triazolium station, alkyl chains as hydrophobic connectors between such units, and hydrophilic stoppers. The moving component consists of a larger crown ether capable of encircling the axle, covalently linked to a smaller crown ether that serves as receptor for potassium ions. The rotaxane was embedded in the membrane of liposomes of about 100 nm diameter, and the ion transport process was investigated by means of fluorescence and NMR spectroscopy experiments performed both on the transporter and on specific model compounds. Taken together, the results are consistent with accelerated K^+ transport across

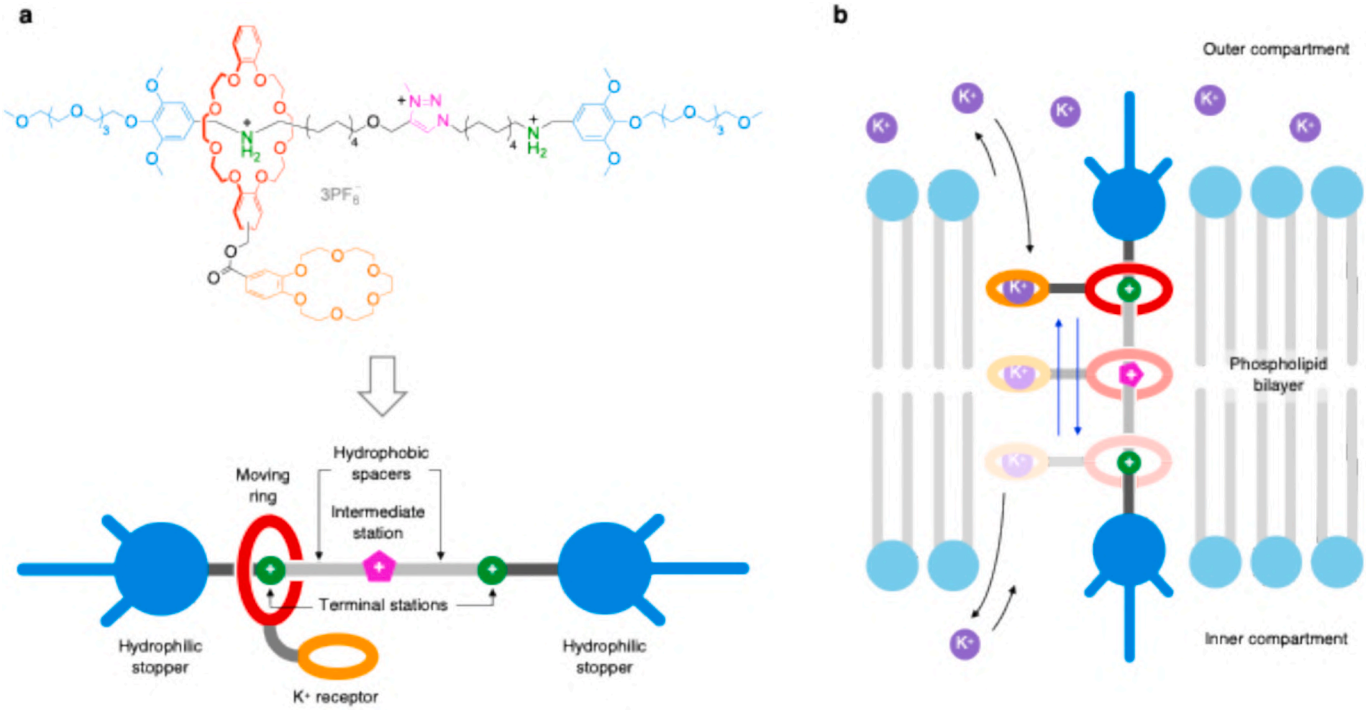

Fig. 13. Structure formula (a) and simplified operation scheme (b) of a membrane-bound rotaxane-based molecular machine capable of exploiting the thermally driven shuttling of its macrocyclic component along the amphiphilic axle to passively carry K^+ ions across the lipid bilayer of a vesicle [119].

the membrane mediated by the macrocyclic component and its stochastic shuttling motion between the terminal ammonium stations, with the central triazolium unit functioning as an intermediate 'relay' station (Fig. 13b) [113]. More recently, a parent rotaxane bearing an azobenzene photoswitch in the center of the axle was investigated with the aim of obtaining light-gated transport [120]. In fact, photoisomerization of the rotaxane from *E* to *Z* was found to lower the efficiency of the transport, an observation that was related to the much slower shuttling rate of the crown ether in the *Z* isomer compared to the *E* isomer. It should be emphasized, however, that in these systems what drives the transport of the cargo is a concentration gradient, which is consumed during operation.

10. Motors

Molecular motors are molecular machines capable of exploiting an energy source to perform repeated directionally controlled movements [2,21,22]. In principle, these mechanical nanoscale devices can perform work on their environment, with a net effect that can be progressively increased as the motor repeats its operation cycle, allowing a task to be performed; in this regard, molecular motors are fundamentally different from mechanical switches. This ability of molecular motors is convincingly and beautifully demonstrated by the biomolecular motors that carry out crucial functions in living organisms [52]. Directionally controlled movements in molecular systems are obtained by exploiting an energy input to rectify random thermal motion, according to mechanisms such as energy ratchet and information ratchet. A discussion of these fundamental aspects of molecular-scale movement is beyond the scope of this article and can be found in the literature [121–123].

As pointed out in the previous sections, MIMs are particularly suitable systems for developing molecular machines, including motors [124,125]. Recent developments in this area include molecular pumps based on rotaxanes and rotary motors based on catenanes.

Molecular pumps are devices capable of moving directionally a molecular or ionic substrate without a concentration gradient or even against it [126]. They must exploit ratchet mechanisms, need energy to operate and should ideally move the substrate across physically separated compartments, so that their repeated action leads to accumulation of the substrate in one compartment, ultimately creating a concentration difference with the other. In the past few years, pseudorotaxane structures have been employed to construct artificial molecular pumps fueled by chemical [127–130], electrical [127,128,131] or light [127,132–134], stimuli. In these systems, the moving substrate is typically a macrocycle, which is collected from a solution and transferred directionally along the axle that serves as a 'track'. If the latter is stoppered at the other extremity, 'impossible' pseudorotaxanes can be created, which store the input energy in the form of their non-equilibrium concentration.

While an extensive discussion of these systems goes beyond the aim of the present review, it is worth noting that, in certain cases, the distinction between pseudorotaxanes and rotaxanes is nuanced, as it depends entirely on the kinetic barrier associated with the unthreading. An example of this concept is represented by the electrochemically-fueled molecular pump shown in Fig. 14 [128] This system is composed by a bis(4,4'-bipyridinium) macrocycle and an axle comprising a 2,6-dimethylpyridinium electrostatic barrier, a 4,4'-bipyridinium unit, an isopropylphenylene steric barrier, and a collecting chain for the rings. In the initial state the macrocycle does not associate with the axle due to electrostatic repulsion; upon reduction of the bipyridinium units, the repulsion becomes weaker and the strong radical-radical interaction between the bipyridinium units of the two components drives the formation of a [2]pseudorotaxane (Fig. 14). Upon subsequent re-oxidation, the macrocycle moves toward the collecting chain instead of unthreading, due to electrostatic repulsion with the positively charged extremity on the axle; at this stage the macrocycle is kinetically trapped due to the electrostatic repulsion, and the systems

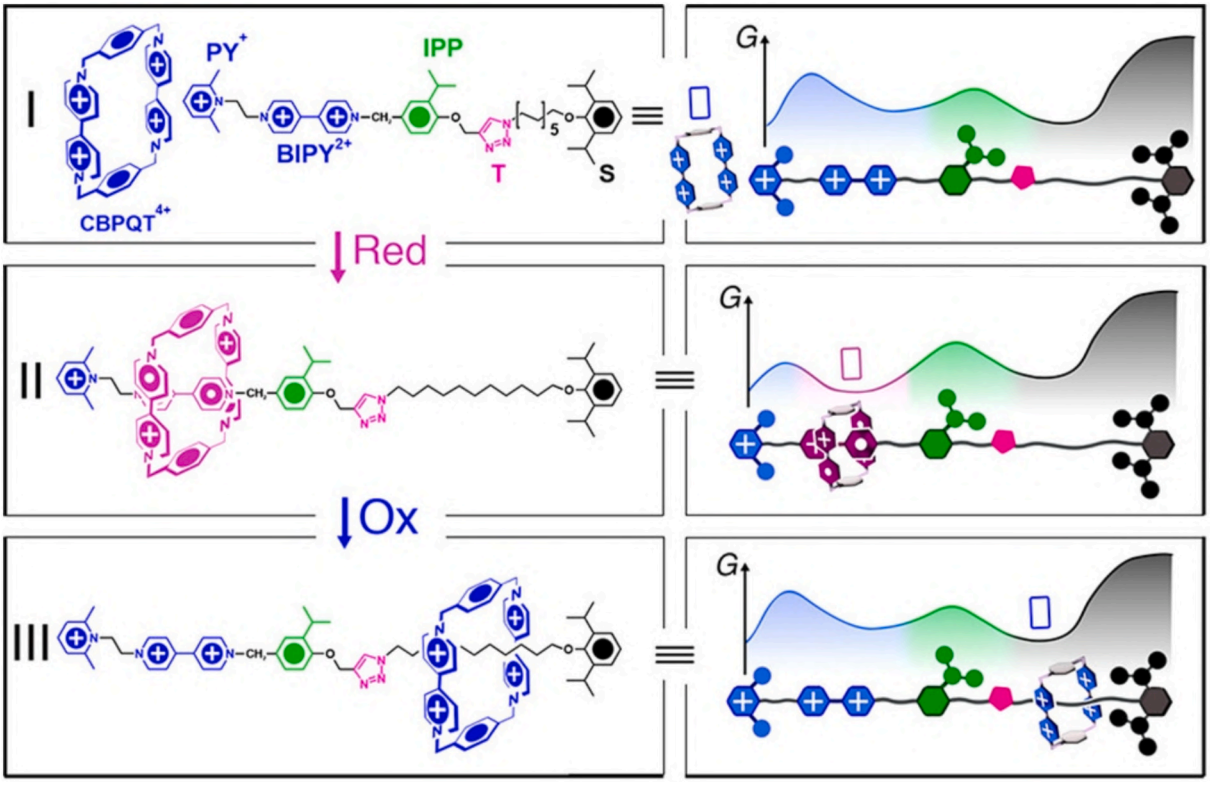

Fig. 14. Structure formulas and operation scheme of an electrochemically-driven molecular pump. (I) In the initial state, the axle and the macrocycle do not interact due to electrostatic repulsion; (II) the reduction of the bipyridinium units triggers the assembly, driven by radical-radical interactions; (III) the re-oxidation of the bipyridinium units induces the ring movement toward the collecting chain. Reproduced with permission from Ref. [129] © 2021 American Chemical Society.

behaves as a [2]rotaxane.

Another design to achieve pumping in [2]rotaxanes relies on using an external energy input to induce the motion of the macrocycle along the axle, driving the distribution of the ring along the axle away from equilibrium [135,136]. Such an outcome is fundamentally different from that of a mechanical switch (Fig. 6a), whose states always correspond to equilibrium structures. A recent chemically driven example is the [2]rotaxane shown in Fig. 15 [135]. It consists of a benzylic amide macrocycle (red) and a stoppered axle containing two identical fumaramide stations (green; one of them is deuterated for analytical purposes) and a carboxylic residue (magenta) positioned between them but closer to one of the two. The macrocycle can freely move between the two equivalent stations by shuttling over the carboxylic moiety, establishing an equilibrium between a proximal co-conformation, in which the ring encircles the station closer to the carboxylic unit, and a distal one, in which the ring encircles the other station (Fig. 15, top). A carbodiimide reactant can activate the carboxylate moiety on the axle, favoring the formation of an ester by nucleophilic attack, which creates a barrier (blue) that prevents the macrocycle from shuttling. Subsequent ester hydrolysis can remove the barrier and resume ring shuttling between the equivalent stations. The rate of barrier removal is faster in the proximal co-conformation because the interaction with the ester through hydrogen bonding activates it towards nucleophilic attack. On the other hand, barrier formation is sterically hindered by the presence of the macrocycle, and therefore it occurs faster in the distal co-conformation. Such a kinetic asymmetry, combined with the catalytic fuel (carbodiimide)-to-waste (urea) conversion, allows the cycle to be repeated and accumulate the distal co-conformation according to an information ratchet mechanism. The chemical fuel is used autonomously by the device, that is, the latter keeps performing its operation cycle as long as unreacted fuel is present, without sequential addition of inputs or other external intervention. It was shown that, under the conditions employed, the distal/proximal ratio changes from 1:1 (equilibrium value) to about 18:1 in the presence of the fuel. The same reaction scheme was later adapted to a [2]catenane to obtain an autonomous chemically driven rotary motor [137]. Examples of [2]rotaxanes capable of autonomously exploiting light energy to populate dissipative states characterized by non-equilibrium distribution of the macrocycle along the axle were also described [138,139].

The first report of an autonomous chemically fueled rotary motor deals with the [2]catenane illustrated in Fig. 16 [140]. The catenane consists of a smaller ring – the same benzylic amide macrocycle (red) of the rotaxane in Fig. 15 – interlocked with a larger ring containing two identical fumaramide stations (green; one of them is deuterated for analytical purposes). The addition of 9-fluorenylmethoxycarbonyl chloride (Fmoc-Cl) creates a barrier (blue) on the larger ring that blocks the thermally driven shuttling of the smaller ring between the two equivalent stations, while cleavage of the bulky substituent restores the motion. The rate of Fmoc removal is independent on the position of the smaller macrocycle, whereas Fmoc attachment is sterically hindered by the latter; as a result, barrier formation occurs faster at the site distant from the smaller ring, thereby introducing steric hindrance to backward motion. Under conditions in which both Fmoc cleavage and attachment can occur, the smaller ring rotates directionally around the larger one; the process goes on as long as Fmoc-Cl is available. In fact, the catenane acts as a catalyst for the decomposition of Fmoc-Cl into dibenzofulvene, CO_2 and HCl, which is the reaction that provides the energy to drive the directional rotation. Previously reported chemically driven catenane rotary motors [141–143], were based on energy ratchet mechanisms and were unable to process the energy inputs autonomously.

A MIM-based rotary motor powered by electrical energy was recently described for the first time [144]. It consists of a [3]catenane (Fig. 17) in which two identical bis(4,4'-bipyridinium) tetracationic macrocycles encircle a larger ring containing a 4,4'-bipyridinium unit (blue), a bis (phenyl)methane moiety (green), another 4,4'-bipyridinium unit, an isopropylphenylene steric barrier (red), a triazole moiety (magenta), and a 2,6-dimethylpyridinium electrostatic barrier (orange), in this sequence, connected by methylene spacers. In the starting (oxidized) state, the two tetracationic rings encircle the triazole and bis(phenyl) methane sites because of the electrostatic repulsion by the bipyridinium units of the larger macrocycle. Upon electrochemical reduction of all the bipyridinium units of the catenane to the radical cationic form (reduced

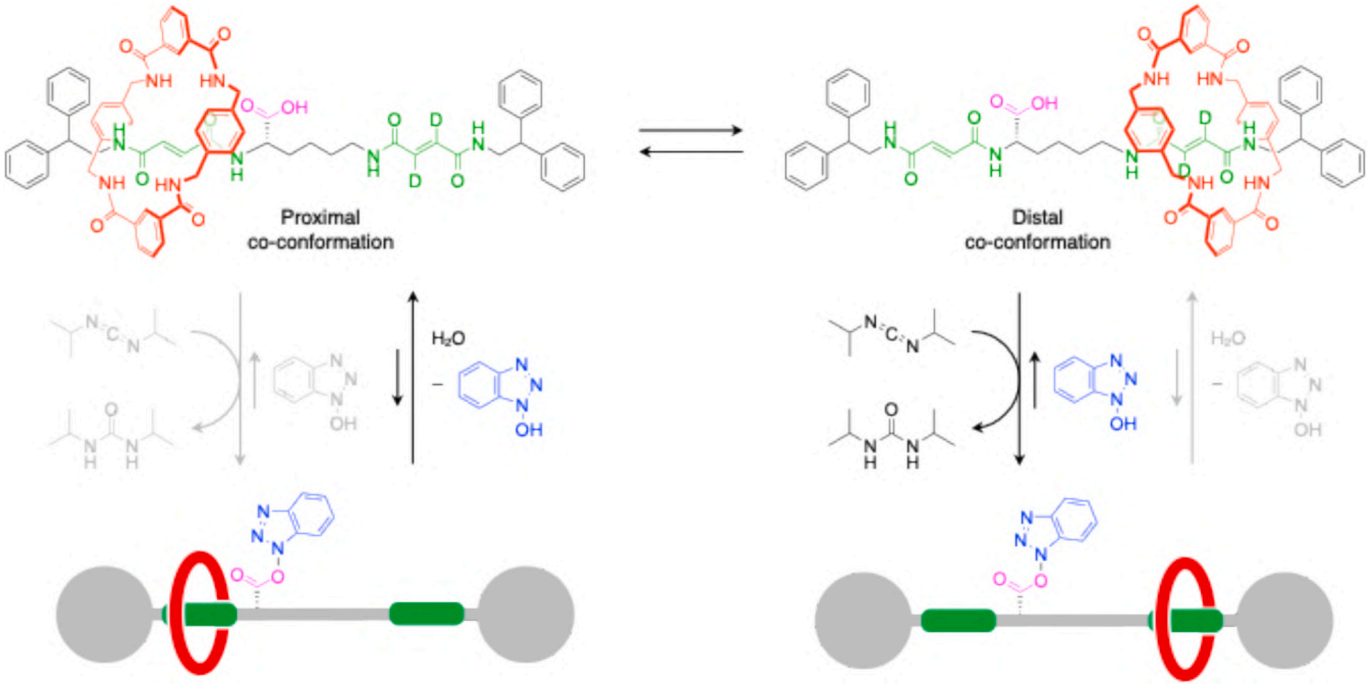

Fig. 15. Structure formula and operation scheme of a [2]rotaxane capable of exploiting a chemical reaction to displace the distribution of the macrocycle between two equivalent recognition sites on the axle away from equilibrium [135]. Key to the operation is the kinetic asymmetry provided by the different rates of both ester formation and hydrolysis depending on the position of the macrocycle, which allows an information ratchet mechanism to be established.

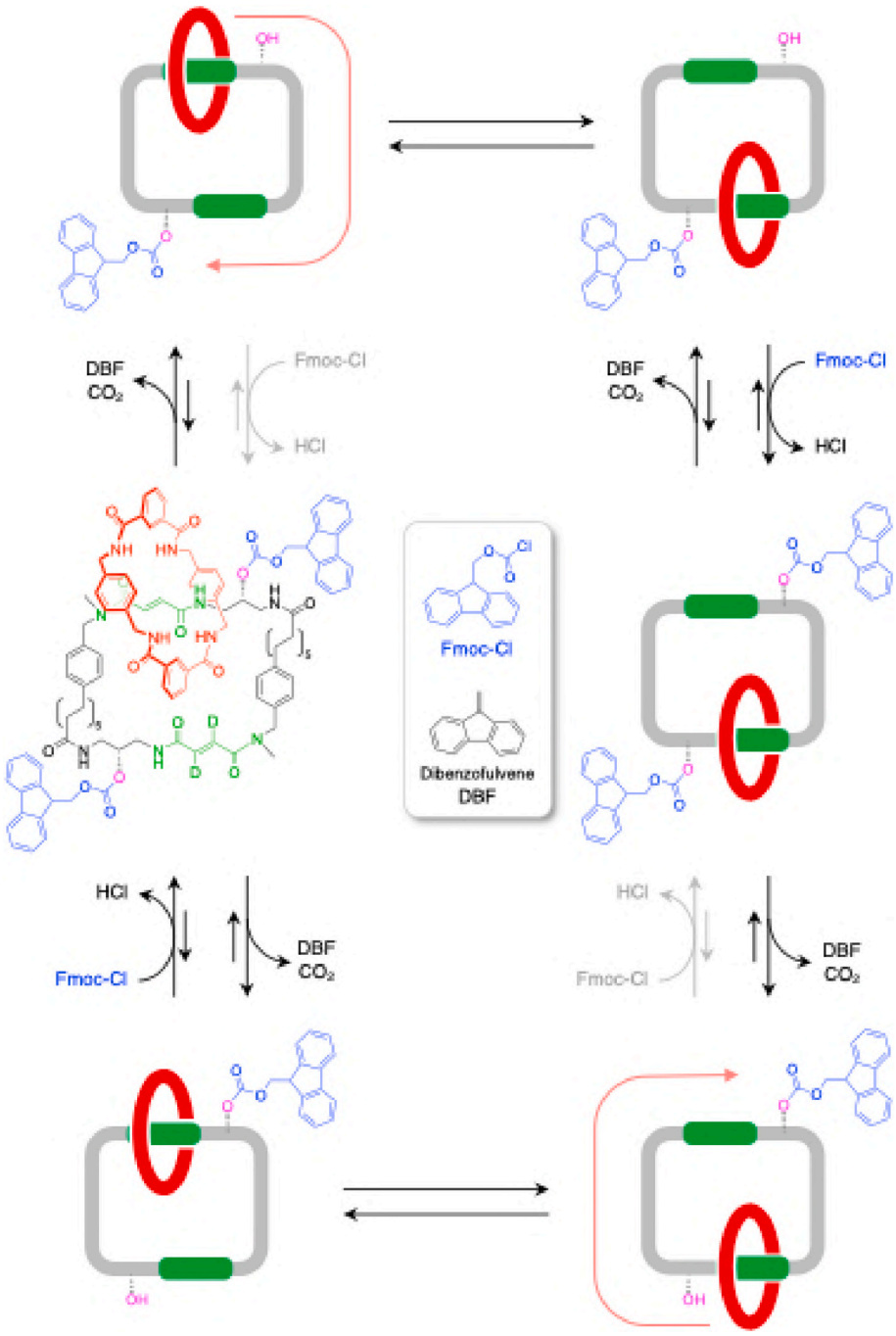

Fig. 16. Structure formula and operation scheme of an autonomous chemically driven molecular rotary motor based on a [2]catenane [140]. The different rates of barrier formation at the hydroxy sites closer and distant from the benzylic amide macrocycle are used to rectify random thermal motion by an information ratchet mechanism, allowing the directional rotation of the smaller ring around the larger one.

state, light blue), strong radical-radical interactions can be established, causing the displacement of the smaller macrocycles on the bipyridinium radical cations of the larger ring. These movements occur with directional preference because in the reduced state the steric barrier is more hindering that the electrostatic one; therefore, the ring encircling the triazole site will overpass the dimethylpyridinium moiety faster than the isopropylphenylene one, determining a preference for clockwise rotation as shown in Fig. 17. The other ring will 'follow the leader' and occupy the other bipyridinium site, also by directional motion. Successive return to the oxidized state, again by electrochemical stimulation, restores the initial binding preference; under these conditions, however, the steric barrier is lower than the electrostatic one and the smaller macrocycles continue to move with the same directional preference as in the previous step. At the end of one reduction-oxidation cycle, the two smaller macrocycles have rotated with high directional preference (ca. 85%) for 180° around the larger one; upon repeating the red-ox cycle, a full 360° directional rotation is achieved. Experiments performed on the parent [2]catenane lacking one smaller ring showed that the presence of the two smaller macrocycles is crucial to observe directionality; this is because, in each 180° step, the motion of one smaller ring prevents the backward displacement of the other. Overall, the electrically powered reduction and oxidation of the [3]catenane creates an energy ratchet mechanism; the motor, however, is not autonomous because the stimulus needs to be periodically changed (from reducing to oxidizing

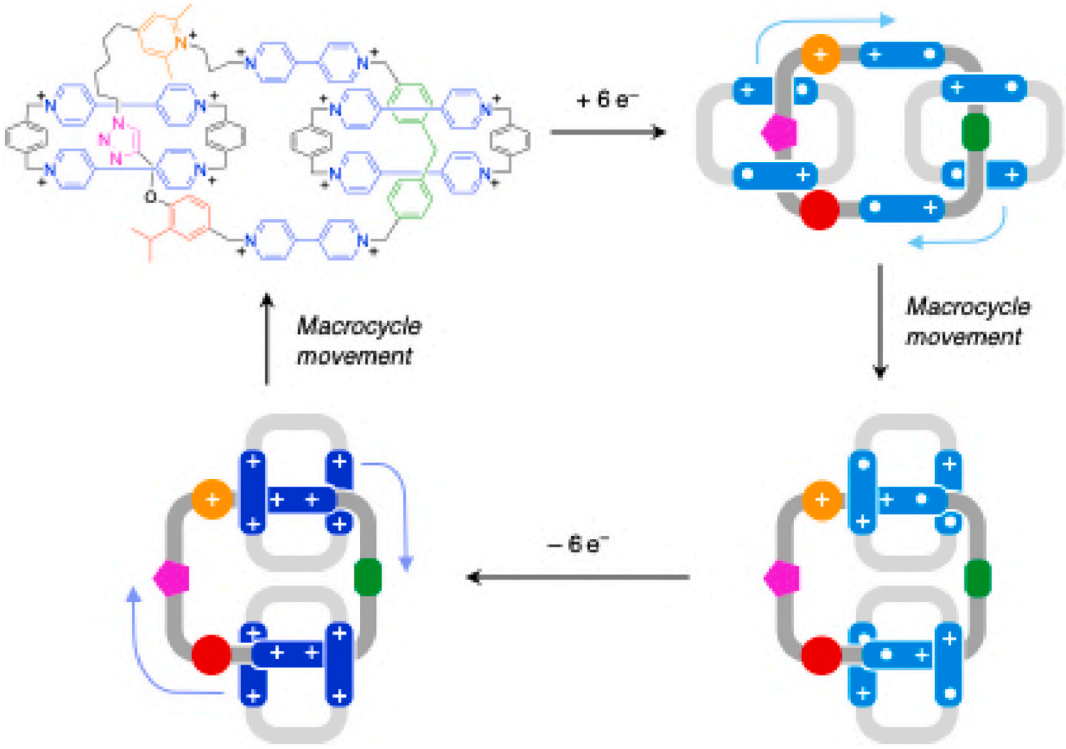

Fig. 17. Structure formula and operation scheme of an electrochemically driven molecular rotary motor based on a [3]catenane [144]. Alternating reduction and oxidation activate an energy ratchet mechanism that enables the 180° directional rotation of the two smaller rings around the larger one; repeating the rex-ox sequence results in a full 360° rotation.

potential values) in a state-dependent manner to performed repeated rotation. The requirements that need to be met to achieve autonomous electrical operation of molecular machines were recently discussed [145] on an experimental system based on pseudorotaxane threading-unthreading [146].

11. Functional materials

The deposition of mechanically interlocked molecular components on solid surfaces, or their incorporation in condensed-phase and solid-state materials, such as polymers [147–151] and metal-organic

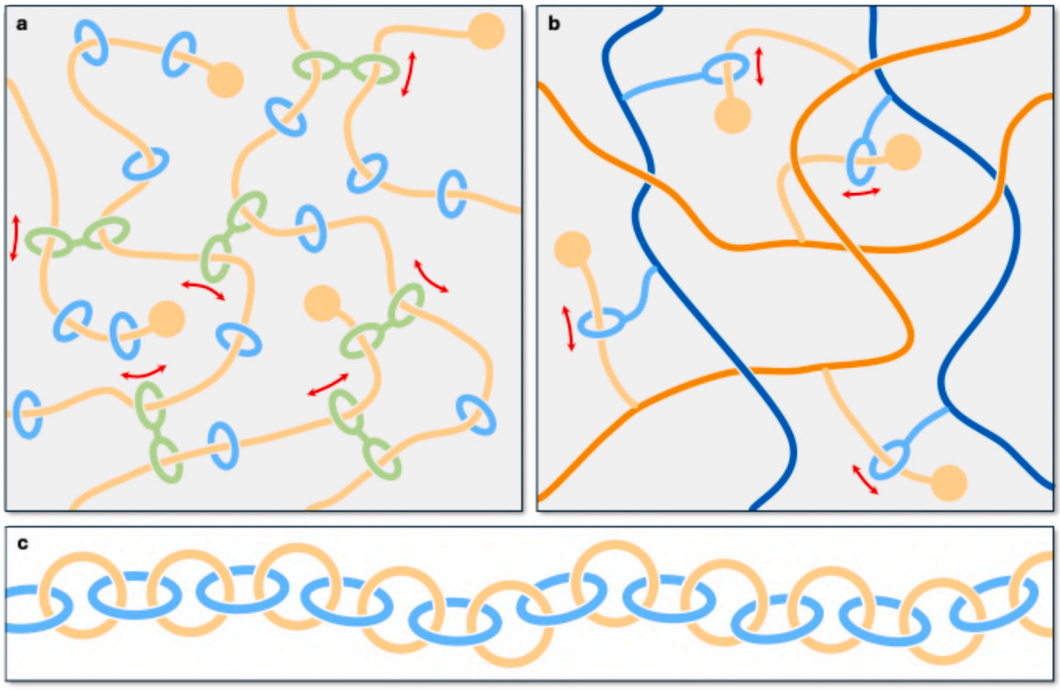

Fig. 18. Schematic representation of different types of mechanically interlocked polymers: (a) slide-ring materials (figure-of-eight components in green); (b) [2] rotaxane crosslinkers; (c) a linear poly[*n*]catenane. The red arrows in (a) and (b) illustrate the pulley effect.

frameworks [152–154], can endow these matrices with unique properties, including adaptability and response to stimuli, coupled with the robustness typical of the mechanical bond. Moreover, such an approach allows to spatially organize a large number of individual molecular devices and exploit collective effects resulting from their synchronous activation [155].

A remarkable example of the integration of mechanical bonds with macromolecular scaffolds is provided by the so-called 'slide-ring materials' [151], in which figure-of-eight cyclodextrin rings mechanically interlocked with polyethylene glycol (PEG) chains create mobile crosslinking sites (Fig. 18a) [156]. The low-barrier sliding motion can provide relaxation pathways to balance the tension of the threaded polymer (pulley effect [151]), resulting in unusual properties such as extreme softness, high stretchability and huge swelling. The mechanical properties of slide-ring materials can be tuned by changing the PEG/cyclodextrin ratio and/or the fraction of covalently connected cyclodextrin rings. The peculiar self-healing and scratch-proofing behavior of these materials favored their application as coatings for automobiles and consumer electronic products [157]. Recently, the slide-ring approach was applied to obtain PEG-type hydrogels with unprecedented toughness, owing to the ability of the interlocked gel to rapidly dissipate the input energy [158].

Another way to harness the pulley effect is to employ [2]rotaxanes as crosslinking units between macromolecular chains (Fig. 18b) [159]. As for the slide-ring gels, the density of the mechanical bonds in the polymer is the main factor determining the mechanical properties of the resulting material [160]. Polymer networks exhibiting a high density of [2]rotaxane crosslinks were found to exhibit superior stretchability, toughness, resistance to puncture and energy dissipation capacity [161]. These materials are also of interest for flexible electronics, as demonstrated by their use in the fabrication of stretchable electroluminescent devices [162].

In the examples presented so far, polymerization was carried out using monomers that already contained the mechanical bond, because forming such a bond during the polymerization step is exceptionally challenging. Perhaps the most exemplary type of mechanically interlocked polymer in which the formation of the mechanical bond is inherent to polymerization is a poly[*n*]catenane (Fig. 18c), with $n>>2$ [163]. These macromolecules contain a very high density of mechanical bonds and can be considered as the molecular equivalent of a macroscopic chain. The degrees of freedom of their structure – both conformational (that is, related to deformation of the individual rings) and co-conformational (that is, related to elongation, rotation and/or twisting of two interlocked rings) – are predicted to endow poly[*n*]catenanes with superior energy damping, toughness and stimuli-responsive behavior. Although the synthesis of polymers of this kind remains a major challenge, the recently reported high-yield preparation of linear, branched and cyclic poly[*n*]catenanes, with *n* comprised between 4 and 130, gives hope for the future development of this extraordinary class of materials [164].

Extending the mechanical bond into higher-dimension architectures represents a major step towards creating materials with emergent, bulk mechanical properties. While most mechanically interlocked polymers are limited to mono dimensional (1D) linear chains, 2D polymers are highly challenging to synthesize because the precise molecular alignment required for interlocking must be maintained across a large, ordered sheet. In a seminal work published very recently, the first example of a 2D mechanically interlocked polymer was achieved [165]. The key innovation was a novel solid-state polymerization method: one set of X-shaped monomers was pre-organized into a highly ordered crystalline lattice, which was then infiltrated and reacted with a second monomer. This reaction simultaneously formed the covalent polymer linkages and the mechanical bonds at each repeat unit, resulting in a chainmail-like layered solid where the interlocked rings provide topological reinforcement. This strategy successfully overcame the challenge of thermal randomization by capitalizing on the precise, ordered environment of the crystal. The resulting polymer is readily exfoliated into individual sheets and, when incorporated into composite fibers, confers enhanced stiffness and strength, demonstrating how the mechanical bond can be leveraged for high-performance functional materials [165].

Moreover, MIMs are attractive platforms to develop mechanophores, i.e., molecules that provide a physico-chemical response to mechanical forces [166]. For example, pulling the macrocyclic ring of a rotaxane away from its axle can modulate the distance between functional units embedded in the interlocked components, and eventually lead to their extrusion – that is, the rupture of the mechanical bond [167]. Such mechanical events can be induced either by high-frequency agitation (sonication) or by incorporating the MIMs into polymer matrices and applying tensile or deformation forces. Despite the complexity of the structures investigated, ^{1}H-NMR spectroscopy proved sufficient to study these systems.

The incorporation of mechanophores in polymers is a promising approach to obtain stimuli-responsive materials [168]. For example, rotaxane-based mechanoluminophores – i.e., molecules whose luminescence properties are modified upon application of an external force – were covalently incorporated into the main chain of polyurethane species to yield materials that reversibly change the intensity of their photoluminescence output in response to mechanical stretching [169–171]. In such system the mechanophore macrocycle typically resides over a quencher incorporated in the axle moiety. The application of mechanical strain on the bulk material results in the mechanophore shuttling away from the quencher, disfavoring the quenching and leading to a measurable increase in emission.

In the examples just described the mechanically interlocked elements play a passive – albeit crucial – role. To move towards active materials, an effective strategy is to link doubly interlocked rotaxane units with a [c2]daisy chain topology in a head-to-tail fashion (Fig. 1b). Such assemblies can undergo reversible extension and contraction when exposed to external stimuli, embodying the so-called 'molecular muscle' concept [172–176]. Functionally, this architecture reproduces the amplification mechanism observed in the myofibrils of skeletal muscles [52]. A notable example of a daisy chain molecular actuator is the compound depicted in Fig. 19a [177]. In acidic conditions, the macrocyclic rings encircle the ammonium sites, resulting in an extended configuration of the molecular muscle; upon increasing the pH, deprotonation of the ammonium sites occurs, prompting the rings to relocate to a secondary binding site – specifically, a triazolium moiety – which drives a contraction of the assembly.

In principle, it is possible to generate a linear polymer by linking together extended daisy chain units (or their deprotonated contracted counterparts), as illustrated in Fig. 19b. Early efforts focused on covalently connecting individual daisy chains end-to-end, but these yielded only short oligomeric species [178]. Subsequent strategies employing coordination chemistry [179] or non-covalent supramolecular methods [180] succeeded in achieving higher degrees of polymerization. These constructs exhibited chemically induced nanoscale extension and contraction along single polymer chains. Later, daisy chains similar to those depicted in Fig. 19a were embedded into branched, covalently bound polymer architectures to produce gels composed of cross-linked networks with stretchable and contractile junctions (Fig. 19c) [181]. Notably, these gels undergo substantial (~50%) and reversible changes in volume in response to pH-driven actuation of the molecular machines. The contraction and expansion of the material can be observed macroscopically (Fig. 19c). Utilization of higher order daisy chain architectures for similar purposes was demonstrated [182]. Chemically switchable daisy chain rotaxanes were also employed to modulate the distance between metal nanoparticles [183].

In another notable example, light-responsive [c2]daisy chain rotaxanes were integrated into polymer matrices to create gels that respond to light in both hydrated and dry states [184]. The polymer (Fig. 20a) was synthesized via polycondensation of α-cyclodextrin–azobenzene [c2] daisy chain rotaxanes [48] with tetra(polyethylene glycol) linkers,

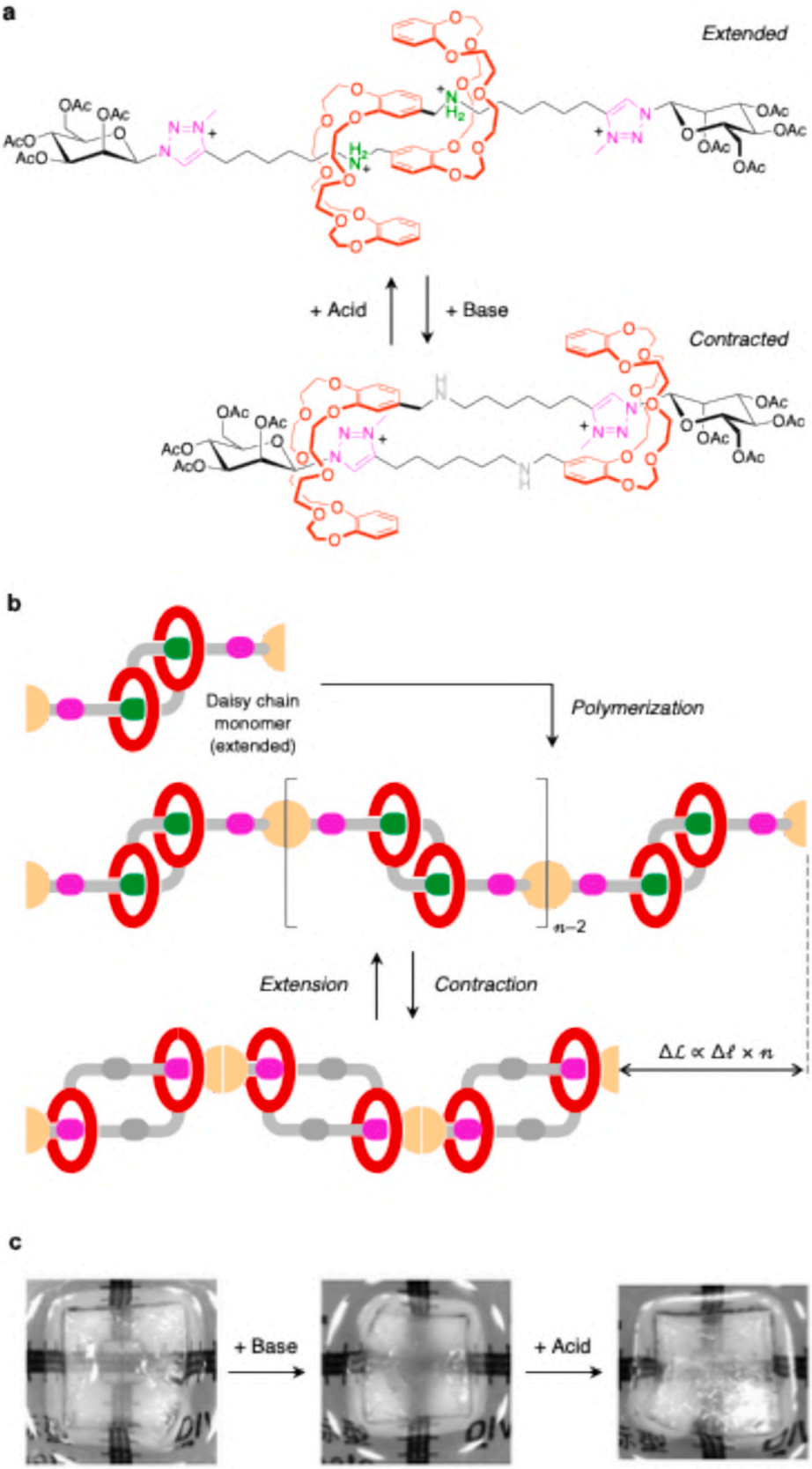

(caption on next page)

Fig. 19. (a) The acid-base-controlled contraction and extension of a [c2]daisy chain rotaxane dimer, a prototype of a 'molecular muscle'. (b) Schematic representation of a linear polymer obtained by polymerization of daisy chain rotaxane dimers. The simultaneous contraction and extension of the monomers can produce an effect on a larger scale; if the macromolecular backbone is sufficiently rigid, its change in length ($\Delta\mathscr{D}$) is proportional to the extent ($\Delta\ell$) of the contraction/extension of the individual monomers and the number (n) of the latter. (c) Photographs of a macroscopic fragment of a crosslinked polymer containing acid-base-switchable molecular muscles in the branches, which show a decrease in the volume of the material when it is immersed in a basic solution; the initial volume is restored upon treatment with an acid solution. Adapted from Ref. [181] © 2017 American Chemical Society.

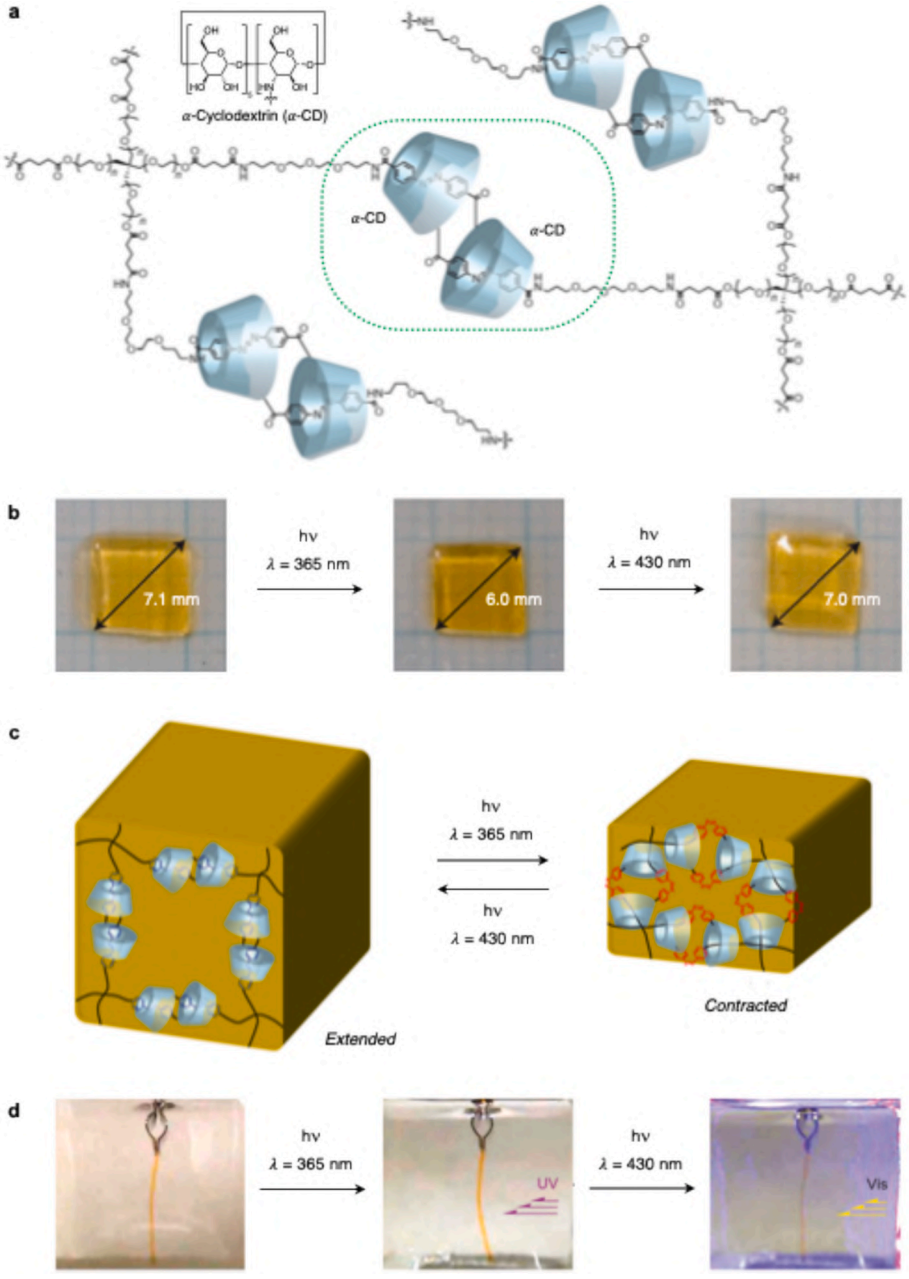

Fig. 20. (a) Chemical formula of a crosslinked polymer incorporating photoresponsive daisy chain units composed of α-cyclodextrin hosts and azobenzene guest molecules (one such unit is highlighted within a dashed oval). The daisy chains are shown in their extended co-conformation, with azobenzene units in the *E*-isomeric form. (b) Photographs of a square hydrogel fragment illustrate its contraction under UV light and subsequent expansion upon exposure to visible light. (c) Diagram outlining the actuation mechanism that underlies the light-induced shape change. (d) Photographs of a hydrogel strip suspended in water and exposed to lateral illumination, demonstrating reversible bending toward the light source. Adapted with permission from Ref. [184] © 2016 Springer Nature.

yielding hydrogel and xerogel materials [185]. UV irradiation caused square-shaped hydrogel samples to shrink, while visible light reversed the effect, restoring their original size (Fig. 20b). This behavior was attributed to reversible $E \rightarrow Z$ and $Z \rightarrow E$ isomerization of the azobenzene units, which respectively drive contraction and extension of the daisy chain components (Fig. 20c). Notably, a control hydrogel containing only azobenzene exhibited opposite behavior: here, *E-Z* isomerization increased the distance between crosslink points. Thus, the two gels rely on distinct mechanisms: in the azobenzene-only system, increased polarity upon isomerization reduces crosslinking density and releases water; in contrast, the daisy chain-based gel changes volume through mechanical adjustment of the length of the molecular machines

(Fig. 20c).

Photoinduced motion was clearly demonstrated by irradiating a gel strip suspended in water (Fig. 20d). Side illumination caused the strip to bend toward the light source due to limited light penetration, which causes activation of the exposed surface only. Maximum bending occurred after 3 hours of UV exposure (365 nm), while reversal with visible light took only minutes. The process was repeatable with no noticeable material degradation.

A remarkable feature of this system, uncommon among polymer actuators, is that light-driven bending persists in the absence of water. A xerogel, prepared by freeze-drying the hydrogel, also bent toward the light, showing a faster response than the hydrated form. However, shape recovery required UV irradiation on the opposite side, and repeated cycling caused a gradual, irreversible size reduction. This quasi-reversible behavior is likely due to the absence of hydrophobic interactions and swelling pressure, both of which help drive α-cyclodextrin shuttling in the hydrated state.

12. Conclusion and outlook

In the last decade, mechanically interlocked molecules (MIMs) have emerged as a promising and versatile platform for the design and construction of functional molecular devices. The mechanical bond, which connects molecular components without requiring strong, direct chemical interactions between them, provides an elegant and effective solution to the challenge of combining structural robustness with dynamic behavior at the molecular scale. As the examples in this review illustrate, this paradigm enables a wide variety of advanced functions, from signal transduction and light harvesting to controlled motion, molecular transport, and the development of responsive materials.

These functions are made possible by the unique dynamic and topological features of interlocked structures like rotaxanes and catenanes, which allow for the relative movement of components while preserving the integrity of the overall assembly. Notably, the field has progressed from fundamental proofs-of-concept to systems exhibiting complex, multi-state switching - such as the modulation of chiroptical activity - and the critically important development of autonomous molecular motors and pumps that consume energy to perform net work. Furthermore, the integration of MIMs into polymers and materials has successfully translated molecular-level motions into macroscopic properties, yielding self-healing gels, exceptionally tough elastomers, and chemically or photochemically actuated materials.

Building upon the remarkable progress achieved, the field now faces several key challenges and opportunities that will determine its future trajectory:

- **Operation under application-relevant conditions.** For the potential of MIM-based devices to be fully realized in technology and medicine, their performance must be robust under complex, real-world conditions. Improving cyclability, response times, and fatigue resistance will be a necessary step to enable practical application in technologies like soft robotics or sensors. Another key objective will be enhancing stability, biocompatibility, and function in aqueous and biologically relevant environments, including bilayer membranes.
- **Mastering non-equilibrium and autonomous operation.** While pioneering examples of autonomous, fueled molecular machines have been reported, mastering dissipative self-assembly remains a central challenge. Future work will need to focus on designing more efficient fuel cycles, also driven by light or electricity, that minimize waste and enable long-term, sustained operation. A deeper understanding of the kinetics governing these non-equilibrium systems is crucial for creating adaptive life-like materials.
- **Towards complex integration and cooperative systems.** The next frontier involves integrating individual MIM-based devices into networked systems capable of performing complex, multi-step tasks. This could entail, for example, coupling an energy-harvesting unit to a molecular machine and a catalytic site to create an artificial metabolic pathway. The integration of MIMs with other nanoscale components, such as biomolecules or electrode surfaces, will also be essential for developing hybrid systems with emergent functionalities.
- **Harnessing collective phenomena.** Despite recent advancements, bridging the gap between the function of individual molecules and their collective behavior remains a significant challenge. Future research will focus on designing MIMs and their supramolecular organizations to facilitate communication and synchronized motion, thereby amplifying molecular-level phenomena to generate coherent macroscopic effects in materials.
- **Advancements through synthesis and characterization.** The pursuit of increasingly complex topologies, such as high molecular weight poly[*n*]catenanes, will continue to drive synthetic innovation. Concurrently, the development of advanced *in situ* and single-molecule characterization techniques will be vital for probing real-time dynamics and elucidating mechanistic details under operational conditions.

In conclusion, the mechanical bond represents not only a structural motif but also a foundational conceptual framework for designing molecular-level functions. By addressing forthcoming challenges, research on mechanically interlocked molecular devices will not only continue to uncover new fundamental science but also pave the way for transformative technologies, from adaptive therapeutics to intelligent, energy-converting materials.

Declaration of competing interest

The authors declare that they have no known competing financial interests or personal relationships that could have appeared to influence the work reported in this paper.

Acknowledgment

Financial support from NextGeneration EU – Mission 4, Component 2, Investment 1.1 (PRIN 2022 project ‘Cosmo’ 2022JMTLE, CUP J53D23008520006) is gratefully acknowledged.

Data availability

No data was used for the research described in the article.

References

[1] The Merriam-Webster English Dictionary, Merriam-Webster Inc., Springfield, Massachusetts, 2022.
[2] V. Balzani, A. Credi, M. Venturi, Molecular Devices and Machines, second ed., Wiley-VCH, Weinheim, 2008.
[3] V. Balzani, A. Credi, M. Venturi, The bottom-up approach to molecular-level devices and machines, Chem. Eur. J. 8 (2002) 5524–5532.
[4] J.-M. Lehn, Supramolecular Chemistry: Concepts and Perspectives, Wiley-VCH, Weinheim, 1995.
[5] J.L. Atwood (Ed.), Comprehensive Supramolecular Chemistry II, Elsevier, Amsterdam, 2017.
[6] S. Bonnet, J.-P. Collin, M. Koizumi, P. Mobian, J.-P. Sauvage, Transition-metal-complexed molecular machine prototypes, Adv. Mater. 18 (2006) 1239–1250.
[7] V. Balzani, G. Bergamini, P. Ceroni, From the photochemistry of coordination compounds to light-powered nanoscale devices and machines, Coord. Chem. Rev. 252 (2008) 2456–2469.
[8] B. Colasson, A. Credi, G. Ragazzon, Light-driven molecular machines based on Ruthenium(II) polypyridine complexes: strategies and recent advances, Coord. Chem. Rev. 325 (2016) 125–134.
[9] M. Nazif Tasbas, E. Sahin, S. Erbas-Cakmak, Bio-inspired molecular machines and their biological applications, Coord. Chem. Rev. 443 (2021) 214039.
[10] M. Venturi, A. Credi, V. Balzani, Electrochemistry of coordination compounds: an extended view, Coord. Chem. Rev. 185-186 (1999) 233–256.
[11] K.T. Mahmudov, M.N. Kopylovich, M.F.C. Guedes da Silvia, A.J.L. Pombeiro, Non-covalent interactions in the synthesis of coordination compounds: recent advances, Coord. Chem. Rev. 345 (2017) 54–72.

[12] J. Zhao, D. Yang, X.-J. Yang, B. Wu, Anion coordination chemistry: from recognition to supramolecular assembly, Coord. Chem. Rev. 378 (2019) 415–444.
[13] J. Owen, The coordination chemistry of nanocrystal surfaces, Science 347 (2015) 615–616.
[14] W.P. Lustig, S. Mukherjee, N.D. Rudd, A.V. Desai, J. Li, S.K. Ghosh, Metal-organic frameworks: functional luminescent and photonic materials for sensing applications, Chem. Soc. Rev. 46 (2017) 3242–3285.
[15] J.-M. Lehn, Supramolecular chemistry - scope and perspectives: molecules, supermolecules, and molecular devices (Nobel Lecture), Angew. Chem. Int. Ed. 27 (1988) 89–112.
[16] See, e.g.: Y. Krishnan, F.C. Simmel, Nucleic acid based molecular devices Angew. Chem. Int. Ed. 50 (2011) 3124–3156.
[17] See, e.g.: F. Lancia, A. Ryabchun, N. Katsonis, Life-like motion driven by artificial molecular machines Nat. Rev. Chem. 3 (2019) 536–551.
[18] See, e.g.; S. Krause, B.L. Feringa, Towards artificial molecular factories from framework-embedded molecular machines, Nat. Rev. Chem. 4 (2020) 550–562.
[19] See, e.g.: E. Del Grosso, E. Franco, L.J. Prins, F. Ricci, Dissipative DNA nanotechnology Nat. Chem. 14 (2022) 600–613.
[20] See, e.g. L. Feng, R.D. Astumian, J.F. Stoddart, Controlling dynamics in extended molecular frameworks Nat. Rev. Chem. 6 (2022) 705–725.
[21] V. Balzani, A. Credi, F.M. Raymo, J.F. Stoddart, Artificial molecular machines, Angew. Chem. Int. Ed. 39 (2000) 3348–3391.
[22] S. Erbas-Cakmak, D.A. Leigh, C.T. McTernan, A.L. Nussbaumer, Artificial molecular machines, Chem. Rev. 115 (2015) 10081–10206.
[23] V. Balzani, A. Credi, M. Venturi, Processing energy and signals by molecular and supramolecular systems, Chem. Eur. J. 14 (2008) 26–39.
[24] N. Le Poul, B. Colasson, Electrochemically and chemically induced redox processes in molecular machines, ChemElectroChem 2 (2015) 475–496.
[25] N. Armaroli, V. Balzani, The future of energy supply: challenges and opportunities, Angew. Chem. Int. Ed. 46 (2007) 52–66.
[26] P. Ceroni, A. Credi, M. Venturi, V. Balzani, Light-powered molecular devices and machines, Photochem. Photobiol. Sci. 9 (2010) 1561–1573.
[27] I.N. Unksov, C.S. Korosec, P. Surendiran, D. Verardo, R. Lyttleton, N.R. Forde, H. Linke, Through the eyes of creators: observing artificial molecular motors, ACS Nanosci. Au 3 (2022) 140–159.
[28] S. Zhang, Y. An, X.-M. Chen, Q. Li, Artificial molecular machines: design and observation, Smart Mol. 1 (2023) e20230015.
[29] C.J. Bruns, J.F. Stoddart, The Nature of the Mechanical Bond: from Molecules to Machines, Wiley, New York, 2016.
[30] J.F. Stoddart, The chemistry of the mechanical bond, Chem. Soc. Rev. 38 (2009) 1802–1820.
[31] R.A.L. Jones, Soft Machines: Nanotechnology and Life, Oxford University Press, Oxford, 2004.
[32] S.R. Beeren, C.T. McTernan, F. Schaufelberger, The mechanical bond in biological systems, Chem 9 (2023) 1378–1412.
[33] J.-P. Sauvage, From chemical topology to molecular machines (Nobel Lecture), Angew. Chem. Int. Ed. 56 (2017) 11080–11093.
[34] H.L. Frisch, E. Wasserman, Chemical topology, J. Am. Chem. Soc. 83 (1961) 3789–3795.
[35] R.S. Forgan, J.-P. Sauvage, J.F. Stoddart, Chemical topology: complex molecular knots, links, and entanglements, Chem. Rev. 111 (2011) 5434–5464.
[36] W. Wang, S. Zhou, X. Yu, Q.-H. Guo, Y. Ma, J. Song, L. Zhang, X. Yan, L. Han, Q. Liao, X. Li, W.-B. Zhang, Y. Mai, S. Zhang, S. Che, H.-B. Yang, X. Fu, M.-X. Wang, What can topology bring to chemistry? CCS Chem. 6 (2024) 2084–2109.
[37] E. Wasserman, The preparation of interlocking rings: a catenane, J. Am. Chem. Soc. 82 (1960) 4433–4434.
[38] G. Schill, A. Lüttringhaus, The preparation of catena compounds by directed synthesis, Angew. Chem. Int. Ed. 3 (1964) 546–547.
[39] C.O. Dietrich-Buchecker, J.-P. Sauvage, Une nouvelle famille de molecules: les metallo-catenanes, Tetrahedron Lett. 24 (1983) 5095–5098.
[40] C.O. Dietrich-Buchecker, J.-P. Sauvage, Interlocking of molecular threads: from the statistical approach to the templated synthesis of catenands, Chem. Rev. 87 (1987) 795–810.
[41] T.J. Hubin, D.H. Busch, Template routes to interlocked molecular structures and orderly molecular entanglements, Coord. Chem. Rev. 200 (2000) 5–52.
[42] J.F. Stoddart, H.-R. Tseng, Chemical synthesis gets a fillip from molecular recognition and self-assembly processes, Proc. Natl. Acad. Sci. U. S. A. 99 (2002) 4797–4800.
[43] J.D. Crowley, S.M. Goldup, A.-L. Lee, D.A. Leigh, R.T. McBurney, Active metal template synthesis of rotaxanes, catenanes and molecular shuttles, Chem. Soc. Rev. 38 (2009) 1530–1541.
[44] M. Denis, S.M. Goldup, Controlling catalyst activity, chemoselectivity and stereoselectivity with the mechanical bond, Nat. Rev. Chem. 1 (2019) 0061.
[45] A. Saura-Sanmartin, C.A. Schalley, Self-sorting as a versatile strategy in the synthesis of rotaxanes and catenanes, Chem 9 (2024) 823–846.
[46] A. Saura-Sanmartin, Synthesis of 'impossible' rotaxanes, Chem. Eur. J. 30 (2024) e202304025.
[47] P. Waelès, M. Gauthier, F. Coutrot, Challenges and opportunities in the post-synthetic modification of interlocked molecules, Angew. Chem. Int. Ed. 60 (2020) 16778–16799.
[48] D.P. Couto, Q. Lin, J.B.M. Whittingham, D.J. Tetlow, J. Zhong, P. Howlader, D. A. Leigh, Multiple template site nitrogen atom deletions from rotaxanes, catenanes, and a molecular knot, J. Am. Chem. Soc. 147 (2025) 33304–33314.
[49] T. Wachsmuth, R. Kluifhooft, M. Müller, L. Zeiss, M. Kathan, A molecular machine directs the synthesis of a catenane, Science 389 (2025) 526–531.
[50] D. Sluysmans, J.F. Stoddart, The burgeoning of mechanically interlocked molecules in chemistry, Trends Chem. 1 (2019) 185–197.
[51] Z. Ashbridge, S.D.P. Fielden, D.A. Leigh, L. Pirvu, F. Schaufelberger, L. Zhang, Knotting matters: orderly molecular entanglements, Chem. Soc. Rev. 51 (2022) 7779–7809.
[52] D.S. Goodsell, The Machinery of Life, second ed., Copernicus, New York, 2009.
[53] M. Albrecht, "Let's twist again": double-stranded, triple-stranded, and circular helicates, Chem. Rev. 101 (2001) 3457–3497.
[54] M. Han, D.M. Engelhard, G.H. Clever, Self-assembled coordination cages based on banana-shaped ligands, Chem. Soc. Rev. 43 (2014) 1848–1860.
[55] J.-F. Ayme, J.E. Beves, C.J. Campbell, D.A. Leigh, Template synthesis of molecular knots, Chem. Soc. Rev. 42 (2013) 1700–1712.
[56] M.M.J. Smulders, I.A. Riddell, C. Browne, J.R. Nitschke, Building on architectural principles for three-dimensional metallosupramolecular construction, Chem. Soc. Rev. 42 (2013) 1728–1754.
[57] D. Fujita, Y. Ueda, S. Sato, N. Mizuno, T. Kumasaka, M. Fujita, Self-assembly of tetravalent Goldberg polyhedra from 144 small components, Nature 540 (2016) 563–566.
[58] V. Balzani, A. Credi, M. Venturi, Controlled disassembling of self-assembling systems: toward artificial molecular-level devices and machines, Proc. Natl. Acad. Sci. USA 99 (2002) 4814–4817.
[59] E.A. Neal, S.M. Goldup, Chemical consequences of mechanical bonding in catenanes and rotaxanes: isomerism, modification, catalysis and molecular machines for synthesis, Chem. Commun. 50 (2014) 5128–5142.
[60] See, e.g. M.-P. Santoni, G.S. Hanan, B. Hasenknopf, Covalent multi-component systems of polyoxometalates and metal complexes: toward multi-functional organic–inorganic hybrids in molecular and material sciences Coord. Chem. Rev. 281 (2014) 64–85.
[61] See, e.g. P.S. Bols, H.L. Anderson, Template-directed synthesis of molecular nanorings and cages Acc. Chem. Res. 51 (2018) 2083–2092.
[62] V. Sundström, Photosynthetic light harvesting, charge separation, and photoprotection: the primary steps, in: L.O. Björn (Ed.), Photobiology: The Science of Light and Life, Springer, New York, 2015, pp. 289–319.
[63] V. Balzani, A. Credi, M. Venturi, Photochemical conversion of solar energy, ChemSusChem 1 (2008) 26–58.
[64] M.J. Llansola-Portoles, D. Gust, T.A. Moore, A.L. Moore, Artificial photosynthetic antennas and reaction centers, C. R. Chimie 20 (2017) 296–313.
[65] A. Adronov, J.M.J. Fréchet, Light-harvesting dendrimers, Chem. Commun. (2000) 1701–1710.
[66] F. Puntoriero, S. Serroni, G. La Ganga, A. Santoro, M. Galletta, F. Nastasi, E. La Mazza, A.M. Cancelliere, S. Campagna, Photo- and redox-active metal dendrimers: a journey from molecular design to applications and self-aggregated systems, Eur. J. Inorg. Chem. (2018) 3887–3899.
[67] V. Balzani, P. Ceroni, A. Juris, M. Venturi, S. Campagna, F. Puntoriero, S. Serroni, Dendrimers based on photoactive metal complexes: recent advances, Coord. Chem. Rev. 219 (2001) 545–572.
[68] G.M. Hübner, G. Nachtsheim, Y.L. Qian, C. Seel, F. Vögtle, the spatial demand of dendrimers: deslipping of rotaxanes, Angew. Chem. Int. Ed. 39 (2000) 1269–1272.
[69] D.B. Amabilino, P.R. Ashton, V. Balzani, C.L. Brown, A. Credi, J.M.J. Fréchet, J. W. Leon, F.M. Raymo, N. Spencer, J.F. Stoddart, M. Venturi, Self-assembly of [n] rotaxanes bearing dendritic stoppers, J. Am. Chem. Soc. 118 (1996) 12012–12020.
[70] J.K. Lee, K. Kim, Rotaxane dendrimers, Top. Curr. Chem. 228 (2003) 111–140.
[71] C.-S. Kwana, K.C.-F. Leung, Development and advancement of rotaxane dendrimers as switchable macromolecular machines, Mater. Chem. Front. 4 (2020) 2825–2844.
[72] X.-Q. Wang, W.-J. Li, W. Wang, H.-B. Yang, Rotaxane dendrimers: alliance between giants, Acc. Chem. Res. 54 (2021) 4091–4106.
[73] W.-J. Li, H. Jiang, X.-Q. Wang, D.-Y. Zhang, Y. Zhu, Y. Ke, W. Wang, H.-B. Yang, Dynamic rotaxane-branched dendrimers with precisely arranged luminogens for efficient light harvesting, Mater. Today Chem. 24 (2022) 100874.
[74] F. Schwer, S. Zank, M. Freiberger, F.M. Steudel, N. Geue, L. Ye, P.E. Barran, T. Drewello, D.M. Guldi, M. von Delius, Nanohoops favour light-induced energy transfer over charge separation in porphyrin/[10]CPP/fullerene rotaxanes, Angew. Chem. Int. Ed. 64 (2025) e202413404.
[75] X. Zhao, G. Wu, B.-T. Liu, H. Han, H. Wu, B. Tang, S. Fang, C. Tang, R. Zhang, S.-N. Lei, E. Liu, Y.-K. X, R.M. Young, M.R. Wasielewski, J.F. Stoddart, Mechanical-bond-enabled highly efficient charge separation in a light-harvesting hetero[2] catenane, J. Am. Chem. Soc. 147 (2025) 28399–28407.
[76] F.-Y. Chen, R. Fu, Z. Gong, C. Li, D.-S. Guo, K. Cai, Ultrahigh-affinity molecular recognition in water and biomedical applications, Angew. Chem. Int. Ed. 64 (2025) e202500916.
[77] J.T. Wilmore, P.D. Beer, Exploiting the mechanical bond effect for enhanced molecular recognition and sensing, Adv. Mater. 36 (2024) 2309098.
[78] See, e.g. M. Denis, J. Pancholi, K. Jobe, M. Watkinson, S.M. Goldup, Chelating rotaxane ligands as fluorescent sensors for metal ions Angew. Chem. Int. Ed. 57 (2018) 5310–5314.
[79] See, e.g. C.G. Collins, E.M. Peck, P.J. Kramera, B.D. Smith, Squaraine rotaxane shuttle as a ratiometric deep-red optical chloride sensor Chem. Sci. 4 (2013) 2557–2563.
[80] H.M. Tay, Y.C. Tse, A. Docker, C. Gateley, A.L. Thompson, H. Kuhn, Z. Zhang, P. D. Beer, Halogen-bonding heteroditopic [2]catenanes for recognition of alkali metal/halide ion pairs, Angew. Chem. Int. Ed. 62 (2023) e202214785.

[81] Y.C. Tse, A. Docker, I. Marques, V. Félix, P.D. Beer, Amphoteric chalcogen-bonding and halogen-bonding rotaxanes for anion or cation recognition, Nat. Chem. 17 (2025) 373–381.
[82] G. Cavallo, P. Metrangolo, T. Pilati, G. Resnati, M. Sansotera, G. Terraneo, Halogen bonding: a general route in anion recognition and coordination, Chem. Soc. Rev. 39 (2010) 3772–3783.
[83] K.T. Mahmudov, A.V. Gurbanov, V.A. Aliyeva, M.F.C. Guedes da Silva, G. Resnati, A.J.L. Pombeiro, Chalcogen bonding in coordination chemistry, Coord. Chem. Rev. 464 (2022) 214556.
[84] J. De Jong, S.J. Wezenberg, A photoswitchable chloride-binding [2]rotaxane, Chem. Eur. J. 31 (2025) e202500461.
[85] J. de Jong, M.A. Siegler, S.J. Wezenber, A photoswitchable [2]catenane receptor, Chem. Commun. 61 (2025) 2548–2551.
[86] R.A. Bissell, E. Cordova, A.E. Kaifer, J.F. Stoddart, A chemically and electrochemically switchable molecular shuttle, Nature 369 (1994) 133–137.
[87] See, e.g. P.R. Ashton, R. Ballardini, V. Balzani, I. Baxter, A. Credi, M.C.T. Fyfe, M. T. Gandolfi, M. Gomez-Lopez, M.-V. Martinez-Diaz, A. Piersanti, N. Spencer, J. F. Stoddart, M. Venturi, A.J.P. White, D.J. Williams, Acid-base controllable molecular shuttles J. Am. Chem. Soc. 120 (1998) 11932–11942.
[88] See, e.g. H. Murakami, A. Kawabuchi, K. Kotoo, M. Kunitake, N. Nakashima, A light-driven molecular shuttle based on a rotaxane J. Am. Chem. Soc. 119 (1997) 7605–7606.
[89] S. Silvi, M. Venturi, A. Credi, Artificial molecular shuttles: from concepts to devices, J. Mater. Chem. 19 (2009) 2279–2294.
[90] X. Ma, H. Tian, Bright functional rotaxanes, Chem. Soc. Rev. 39 (2010) 70–80.
[91] B. Yao, H. Sun, L. Yang, S. Wang, X. Liu, Recent progress in light-driven molecular shuttles, Front. Chem. 9 (2022) 832735.
[92] See, e.g. A. Livoreil, C.O. Dietrich-Buchecker, J.-P. Sauvage, Electrochemically triggered swinging of a [2]-catenate J. Am. Chem. Soc. 116 (1994) 9399–9400.
[93] See, e.g. M. Asakawa, P.R. Ashton, V. Balzani, A. Credi, C. Hamers, G. Mattersteig, M. Montalti, A.N. Shipway, N. Spencer, J.F. Stoddart, M.S. Tolley, M. Venturi, A. J.P. White, D.J. Williams, A chemically and electrochemically switchable [2] catenane incorporating a tetrathiafulvalene unit Angew. Chem. Int. Ed. 37 (1998) 333–337.
[94] See, e.g. J.D. Badjic, V. Balzani, A. Credi, S. Silvi, J.F. Stoddart, A molecular elevator Science 303 (2004) 1845–1849.
[95] See, e.g. F. Durola, V. Heitz, F. Reviriego, C. Roche, J.-P. Sauvage, A. Sour, Y. Trolez, Cyclic [4]rotaxanes containing two parallel porphyrinic plates: toward switchable molecular receptors and compressors Acc. Chem. Res. 47 (2014) 633–645.
[96] See, e.g. G. Ragazzon, C. Schäfer, P. Franchi, S. Silvi, B. Colasson, M. Lucarini, A. Credi, Remote electrochemical modulation of pKa in a rotaxane by co-conformational allostery Proc. Natl. Acad. Sci. U.S.A. 115 (2018) 9385–9390.
[97] S. Corra, C. de Vet, J. Groppi, M. La Rosa, S. Silvi, M. Baroncini, A. Credi, Chemical on/off switching of mechanically planar chirality and chiral anion recognition in a [2]rotaxane molecular shuttle, J. Am. Chem. Soc. 141 (2019) 9129–9133.
[98] E.M.G. Jamieson, F. Modicom, S.M. Goldup, Chirality in rotaxanes and catenanes, Chem. Soc. Rev. 47 (2018) 5266–5311.
[99] A.H.G. David, J.F. Stoddart, Chiroptical properties of mechanically interlocked molecules, Isr. J. Chem. 61 (2021) 608–621.
[100] A.H.G. David, R. Casares, J.M. Cuerva, A.G. Campaña, V. Blanco, A [2]rotaxane-based circularly polarized luminescence switch, J. Am. Chem. Soc. 141 (2019) 18064–18074.
[101] Y. Wang, J. Gong, X. Wang, W.-J. Li, X.-Q. Wang, X. He, W. Wang, H.-B. Wang, Multistate circularly polarized luminescence switching through stimuli-induced co-conformation regulations of pyrene-functionalized topologically chiral [2] catenane, Angew. Chem. Int. Ed. 61 (2022) e202210542.
[102] G. Bottari, F. Dehez, D.A. Leigh, P.J. Nash, E.M. Pérez, J.K. Wong, F. Zerbetto, Entropy-driven translational isomerism: a tristable molecular shuttle, Angew. Chem. Int. Ed. 42 (2003) 5886–5889.
[103] Z. Meng, J.-F. Xiang, C.-F. Chen, Tristable [*n*]rotaxanes: from molecular shuttle to molecular cable car, Chem. Sci. 5 (2014) 1520–1525.
[104] L. Andreoni, J. Groppi, O. Seven, M. Baroncini, A. Credi, S. Silvi, Directional ring translocation in a pH- and redox-driven tristable [2]rotaxane, Angew. Chem. Int. Ed. 64 (2025) e202414609.
[105] M. Baroncini, A. Credi, Gearing up molecular rotary motors, Science 356 (2017) 906–907.
[106] Pioneering work: H. Iwamura, K. Mislow, Stereochemical consequences of dynamic gearing Acc. Chem. Res. 21 (1988) 175–182.
[107] I. Liepuoniute, M.J. Jellen, M.A. Garcia-Garibay, Correlated motion and mechanical gearing in amphidynamic crystalline molecular machines, Chem. Sci. 11 (2020) 12994–13007.
[108] S. Corra, C. de Vet, M. Baroncini, A. Credi, S. Silvi, Stereodynamics of *E/Z* isomerization in rotaxanes through mechanical shuttling and covalent bond rotation, Chem 7 (2021) 2137–2150.
[109] K. Zhu, G. Baggi, S.J. Loeb, Ring-through-ring molecular shuttling in a saturated [3]rotaxane, Nat. Chem. 10 (2018) 625–630.
[110] P. Štacko, J.C.M. Kistemaker, T. van Leeuwen, M.C. Chang, E. Otten, B.L. Feringa, Locked synchronous rotor motion in a molecular motor, Science 356 (2017) 964–968.
[111] J.-J. Yu, L.-Y. Zhao, Z.-T. Shi, Q. Zhang, G. London, W.-J. Liang, C. Gao, M.-M. Li, X.-M. Cao, H. Tian, B.L. Feringa, D.-H. Qu, Pumping a ring-sliding molecular motion by a light-powered molecular motor, J. Org. Chem. 84 (2019) 5790–5802.
[112] S. Matile, T. Fyles, Transport across membranes, Acc. Chem. Res. 46 (2013) 2741–2742.
[113] A. Credi, A molecular cable car for transmembrane ion transport, Angew. Chem. Int. Ed. 58 (2019) 4108–4110.
[114] C. Schäfer, G. Ragazzon, B. Colasson, M. La Rosa, S. Silvi, A. Credi, An artificial molecular transporter, ChemistryOpen 5 (2016) 120–124.
[115] S. Bonnet, J.-P. Collin, Ruthenium-based light-driven molecular machine prototypes: synthesis and properties, Chem. Soc. Rev. 37 (2008) 1207–1217.
[116] D. Thomas, D.J. Tetlow, Y. Ren, S. Kassem, U. Karaca, D.A. Leigh, Pumping between phases with a pulsed-fuel molecular ratchet, J. Am. Chem. Soc. 17 (2022) 701–707.
[117] L. Feng, Y. Qiu, Q.-H. Guo, Z. Chen, J.S.W. Seale, K. He, H. Wu, Y. Feng, O. K. Farha, R.D. Astumian, J.F. Stoddart, Active mechanisorption driven by pumping cassettes, Science 374 (2021) 1215–1221.
[118] M.A. Watson, S.L. Cockroft, Man-made molecular machines: membrane bound, Chem. Soc. Rev. 45 (2016) 6118–6129.
[119] S. Chen, Y. Wang, T. Nie, C. Bao, C. Wang, T. Xu, Q. Lin, D.-H. Qu, X. Gong, Y. Yang, L. Zhu, H. Tian, An artificial molecular shuttle operates in lipid bilayers for ion transport, J. Am. Chem. Soc. 140 (2018) 17992–17998.
[120] C. Wang, S. Wang, H. Yang, X. Xiang, X. Wang, C. Bao, L. Zhu, H. Tian, D.-H. Qu, A light-operated molecular cable car for gated ion transport, Angew. Chem. Int. Ed. 60 (2021) 14836–14840.
[121] T. Sangchai, S. Al Shehimy, E. Penocchio, G. Ragazzon, Artificial molecular ratchets: tools enabling endergonic processes, Angew. Chem. Int. Ed. 62 (2023) e202309501.
[122] S. Borsley, D.A. Leigh, B.M.W. Roberts, Molecular ratchets and kinetic asymmetry: giving chemistry direction, Angew. Chem. Int. Ed. 63 (2024) e202400495.
[123] M.P. Leighton, D.A. Sivak, Flow of energy and information in molecular machines, Annu. Rev. Phys. Chem. 76 (2025) 379–403.
[124] S. Kassem, T. van Leeuwen, A.S. Lubbe, M.R. Wilson, B.L. Feringa, D.A. Leigh, Artificial molecular motors, Chem. Soc. Rev. 46 (2017) 2592–2621.
[125] M. Baroncini, S. Silvi, A. Credi, Photo- and redox-driven artificial molecular motors, Chem. Rev. 120 (2020) 200–268.
[126] Y. Qiu, Y. Feng, Q.-H. Guo, R.D. Astumian, J.F. Stoddart, Pumps through the Ages, Chem 6 (2020) 1952–1977.
[127] H. Li, C. Cheng, P.R. McGonigal, A.C. Fahrenbach, M. Frasconi, W.-G. Liu, Z. Zhu, Y. Zhao, C. Ke, J. Lei, R.M. Young, S.M. Dyar, D.T. Co, Y.-W. Yang, Y.Y. Botros, W. A. Goddard III, M.R. Wasielewski, R.D. Astumian, J.F. Stoddart, Relative unidirectional translation in an artificial molecular assembly fueled by light, J. Am. Chem. Soc. 135 (2013) 18609–18620.
[128] C. Cheng, P.R. McGonigal, S.T. Schneebeli, H. Li, N.A. Vermeulen, C. Ke, J. F. Stoddart, An artificial molecular pump, Nat. Nanotechnol. 10 (2015) 547–553.
[129] Y. Feng, M. Ovalle, J.S.W. Seale, C.K. Lee, D.J. Kim, R.D. Astumian, J.F. Stoddart, Molecular pumps and motors, J. Am. Chem. Soc. 143 (15) (2021) 5569–5591.
[130] S. Amano, S.D.P. Fielden, D.A. Leigh, A catalysis-driven artificial molecular pump, Nature 596 (2021) 529–534.
[131] C. Pezzato, M.T. Nguyen, D.J. Kim, O. Anamimoghadam, L. Mosca, J.F. Stoddart, Controlling dual molecular pumps electrochemically, Angew. Chem. Int. Ed. 57 (2018) 9325–9329.
[132] G. Ragazzon, M. Baroncini, S. Silvi, M. Venturi, A. Credi, Light-powered autonomous and directional molecular motion of a dissipative self-assembling system, Nat. Nanotechnol. 10 (2015) 70–75.
[133] S. Corra, L. Casimiro, M. Baroncini, J. Groppi, M. La Rosa, M. Tranfić Bakić, S. Silvi, A. Credi, Artificial supramolecular pumps powered by light, Chem. Eur. J. 27 (2021) 11076–11083.
[134] M. Canton, J. Groppi, L. Casimiro, S. Corra, M. Baroncini, S. Silvi, A. Credi, Second-generation light-fueled supramolecular pump, J. Am. Chem. Soc. 143 (2021) 10890–10894.
[135] S. Borsley, D.A. Leigh, B.M.W. Roberts, A doubly kinetically-gated information ratchet autonomously driven by carbodiimide hydration, J. Am. Chem. Soc. 143 (2021) 4414–4420.
[136] S. Borsley, D.A. Leigh, B.M.W. Roberts, I.J. Vitorica-Yrezabal, Tuning the force, speed, and efficiency of an autonomous chemically fueled information ratchet, J. Am. Chem. Soc. 144 (2022) 17241–17248.
[137] J.M. Gallagher, B.M.W. Roberts, S. Borsley, D.A. Leigh, Conformational selection accelerates catalysis by an organocatalytic molecular motor, Chem 10 (2024) 855–866.
[138] V. Serreli, C.F. Lee, E.R. Kay, D.A. Leigh, A molecular information ratchet, Nature 445 (2007) 523–527.
[139] F. Nicoli, M. Curcio, M. Tranfić Bakić, E. Paltrinieri, S. Silvi, M. Baroncini, A. Credi, Photoinduced autonomous nonequilibrium operation of a molecular shuttle by combined isomerization and proton transfer through a catalytic pathway, J. Am. Chem. Soc. 144 (2022) 10180–10185.
[140] M.R. Wilson, J. Solà, A. Carlone, S.M. Goldup, N. Lebrasseur, D.A. Leigh, An autonomous chemically fuelled small-molecule motor, Nature 534 (2016) 235–240.
[141] D.A. Leigh, J.K.Y. Wong, F. Dehez, F. Zerbetto, Unidirectional rotation in a mechanically interlocked molecular rotor, Nature 424 (2003) 174–179.
[142] J.V. Hernández, E.R. Kay, D.A. Leigh, A reversible synthetic rotary molecular motor, Science 306 (2004) 1532–1537.
[143] A. Li, Z. Du, S. Zhang, J. Xie, X. Li, Q. Chen, Y. Tang, J. Chen, K. Zhu, A compact chemically driven [2]catenane rotary motor operated through alternate pumping and discharging, Chem. Sci. 15 (2024) 14721–14725.
[144] L. Zhang, Y. Qiu, W.-G. Liu, H. Chen, D. Shen, B. Song, K. Cai, H. Wu, Y. Jiao, Y. Feng, J.S.W. Seale, C. Pezzato, J. Tian, Y. Tan, X.-Y. Chen, Q.-H. Guo, C. L. Stern, D. Philp, R.D. Astumian, W.A. Goddard III, J.F. Stoddart, An electric molecular motor, Nature 613 (2023) 280–286.

[145] E. Penocchio, A. Bachir, A. Credi, R.D. Astumian, G. Ragazzon, Analysis of kinetic asymmetry in a multi-cycle reaction network establishes the principles for autonomous compartmentalized molecular ratchets, Chem 10 (2024) 3644–3655.
[146] G. Ragazzon, M. Malferrari, A. Arduini, A. Secchi, S. Rapino, S. Silvi, A. Credi, Autonomous non-equilibrium self-assembly and molecular movements powered by electrical energy, Angew. Chem. Int. Ed. 62 (2023) e202214265.
[147] F.M. Raymo, J.F. Stoddart, Interlocked macromolecules, Chem. Rev. 99 (1999) 1643–1664.
[148] L.F. Hart, J.E. Hertzog, P.M. Rauscher, B.W. Rawe, M.M. Tranquilli, S.J. Rowan, Material properties and applications of mechanically interlocked polymers, Nat. Rev. Mater. 6 (2021) 508–530.
[149] L. Chen, X. Sheng, G. Li, F. Huang, Mechanically interlocked polymers based on rotaxanes, Chem. Soc. Rev. 51 (2022) 7046–7065.
[150] Z. Zhang, J. Zhao, X. Yan, Mechanically interlocked polymers with dense mechanical bonds, Acc. Chem. Res. 57 (2024) 992–1006.
[151] S. Ando, K. Ito, Recent progress and future perspective in slide-ring based polymeric materials, Macromolecules 58 (2025) 2157–2177.
[152] H. Deng, M.A. Olson, J.F. Stoddart, O.M. Yaghi, Robust dynamics, Nat. Chem. 2 (2010) 439–443.
[153] V.N. Vukotic, K.J. Harris, K. Zhu, R.W. Schurko, S.J. Loeb, Metal–organic frameworks with dynamic interlocked components, Nat. Chem. 4 (2012) 456–460.
[154] A. Saura-Sanmartin, A. Pastor, A. Martinez-Cuezva, G. Cutillas-Font, M. Alajarin, J. Berna, Mechanically interlocked molecules in metal–organic frameworks, Chem. Soc. Rev. 51 (2022) 4949–4976.
[155] D. Dattler, G. Fuks, J. Heiser, E. Moulin, A. Perrot, X. Yao, N. Giuseppone, Design of collective motions from synthetic molecular switches, rotors, and motors, Chem. Rev. 120 (2020) 310–433.
[156] Y. Okumura, K. Ito, The polyrotaxane gel: a topological gel by figure-of-eight cross-links, Adv. Mater. 13 (2001) 485–487.
[157] Y. Noda, Y. Hayashi, K. Ito, From topological gels to slide-ring materials, J. Appl. Polym. Sci. 131 (2014) 40509.
[158] C. Liu, N. Morimoto, L. Jiang, S. Kawahara, T. Noritomi, H. Yokoyama, K. Mayumi, K. Ito, Tough hydrogels with rapid self-reinforcement, Science 372 (2021) 1078–1081.
[159] J. Sawada, D. Aoki, S. Uchida, H. Otsuka, T. Takata, Synthesis of vinylic macromolecular rotaxane cross-linkers endowing network polymers with toughness, ACS Macro Lett. 4 (2015) 598–601.
[160] J. Sawada, D. Aoki, H. Otsuka, T. Takata, A guiding principle for strengthening crosslinked polymers: synthesis and application of mobility-controlling rotaxane crosslinkers, Angew. Chem. Int. Ed. 58 (2019) 2765–2768.
[161] X. Yang, L. Cheng, Z. Zhang, J. Zhao, R. Bai, Z. Guo, W. Yo, X. Yan, Amplification of integrated microscopic motions of high-density [2]rotaxanes in mechanically interlocked networks, Nat. Commun. 13 (2022) 6654.
[162] C. Wang, B. Gao, K. Xue, W. Wang, J. Zhao, R. Bai, T. Yun, Z. Fan, M. Yang, Z. Zhang, Z. Zhang, X. Yan, Stretchable [2]rotaxane-bridged MXene films applicable for electroluminescent devices, Sci. Adv. 11 (2025) eadt8262.
[163] G. Liu, P.M. Rauscher, B.W. Rawe, M.M. Tranquilli, S.J. Rowan, Polycatenanes: synthesis, characterization, and physical understanding, Chem. Soc. Rev. 51 (2022) 4928–4948.
[164] Q. Wu, P.M. Rauscher, X. Lang, R.J. Wojtecki, J.J. de Pablo, M.J.A. Hore, S. J. Rowan, Poly[n]catenanes: synthesis of molecular interlocked chains, Science 358 (2017) 1434–1439.
[165] M.I. Bardot, C.W. Weyhrich, Z. Shi, M. Traxler, C.L. Stern, J. Cui, D.A. Muller, M. L. Becker, W.R. Dichtel, Mechanically interlocked two-dimensional polymers, Science 387 (2025) 264–269.
[166] G. De Bo, Mechanochemistry of the mechanical bond, Chem. Sci. 9 (2018) 15–21.
[167] See, e.g. L. Chen, R. Nixon, G. De Bo, Force-controlled release of small molecules with a rotaxane actuator Nature 628 (2024) 320–325.
[168] T. Gridneva, J.R. Khusnutdinova, Functional coordination compounds for mechanoresponsive polymers, Chem. Commun. 61 (2025) 441–454.
[169] Y. Sagara, M. Karman, E. Verde-Sesto, K. Matsuo, Y. Kim, N. Tamaoki, C. Weder, Rotaxanes as mechanochromic fluorescent force transducers in polymers, J. Am. Chem. Soc. 140 (2018) 1584–1587.
[170] Y. Sagara, M. Karman, A. Seki, M. Pannipara, N. Tamaoki, C. Weder, Rotaxane-based mechanophores enable polymers with mechanically switchable white photoluminescence, ACS Cent. Sci. 5 (2019) 874–881.
[171] T. Muramatsu, S. Shimizu, J.M. Clough, C. Weder, Y. Sagara, Force-induced shuttling of rotaxanes controls fluorescence resonance energy transfer in polymer hydrogels, ACS Appl. Mater. Interfaces 15 (2023) 8502–8509.
[172] E. Moulin, C.C. Carmona-Vargas, N. Giuseppone, Daisy chain architectures: from discrete molecular entities to polymer materials, Chem. Soc. Rev. 52 (2023) 7333–7358.
[173] M.C. Jimenez, C. Dietrich-Buchecker, J.-P. Sauvage, Towards synthetic molecular muscles: contraction and stretching of a linear rotaxane dimer, Angew. Chem. Int. Ed. 39 (2000) 3284–3287.
[174] R.E. Dawson, S.F. Lincoln, C.J. Easton, The foundation of a light driven molecular muscle based on stilbene and α-cyclodextrin, Chem. Commun. (2008) 3980–3982.
[175] C.J. Bruns, J.F. Stoddart, Rotaxane-based molecular muscles, Acc. Chem. Res. 47 (2014) 2186–2199.
[176] A. Goujon, E. Moulin, G. Fuks, N. Giuseppone, [c2]Daisy chain rotaxanes as molecular muscles, CCS Chem. 1 (2019) 83–96.
[177] F. Coutrot, C. Romuald, E. Busseron, A new pH-switchable dimannosyl[c2]daisy chain molecular machine, Org. Lett. 10 (2008) 3741–3744.
[178] L. Fang, M. Hmadeh, J. Wu, M.A. Olson, J.M. Spruell, A. Trabolsi, Y.W. Yang, M. Elhabiri, A.M. Albrecht-Gary, J.F. Stoddart, Acid-base actuation of [c2]daisy chains, J. Am. Chem. Soc. 131 (2009) 7126–7134.
[179] G. Du, E. Moulin, N. Jouault, E. Buhler, N. Giuseppone, Muscle-like supramolecular polymers: integrated motion from thousands of molecular machines, Angew. Chem. Int. Ed. 51 (2012) 12504–12508.
[180] A. Goujon, G. Du, E. Moulin, G. Fuks, M. Maaloum, E. Buhler, N. Giuseppone, Hierarchical self-assembly of supramolecular muscle-like fibers, Angew. Chem. Int. Ed. 55 (2016) 703–707.
[181] A. Goujon, T. Lang, G. Mariani, E. Moulin, G. Fuks, J. Raya, E. Buhler, N. Giuseppone, Bistable [c2]daisy chain rotaxanes as reversible muscle-like actuators in mechanically active gels, J. Am. Chem. Soc. 139 (2017) 14825–14828.
[182] J.-C. Chang, S.-H. Tseng, C.-C. Lai, Y.-H. Liu, S.-M. Peng, S.-H. Chiu, Mechanically interlocked daisy-chain-like structures as multidimensional molecular muscles, Nat. Chem. 9 (2017) 128–134.
[183] Q. Zhang, S.-J. Rao, T. Xie, X. Li, T.-Y. Xu, D.-W. Li, D.-H. Qu, Y.-T. Long, H. Tian, Muscle-like artificial molecular actuators for nanoparticles, Chem 4 (2018) 2679–2684.
[184] K. Iwaso, Y. Takashima, A. Harada, Fast response dry-type artificial molecular muscles with [c2]daisy chains, Nat. Chem. 8 (2016) 625–632.
[185] Y. Takashima, S. Hatanaka, M. Otsubo, M. Nakahata, T. Kakuta, A. Hashidzume, H. Yamaguchi, A. Harada, Expansion-contraction of photoresponsive artificial muscle regulated by host–guest interactions, Nat. Commun. 3 (2012) 1270.